# A quantitative comparison of spaceborne spectrometry and polarimetry measurements of the aerosol direct radiative effect over clouds

Ruben Schulte

# Geoscience and Remote Sensing: Internship project at KNMI

## A quantitative comparison of spaceborne spectrometry and polarimetry measurements of the aerosol direct radiative effect over clouds

*25 September 2016*

*Written by:*
*Ruben B. Schulte*
*Student number: 4009045*

**Supervised by:**
**KNMI: Martin de Graaf**
**Delft University of Technology: Tim Vlemmix**
**Delft University of Technology: John Baggen**

# Abstract

This paper describes a comparison of the aerosol direct radiative effect (DRE), retrieved by two methods on smoke above clouds in the South East Atlantic in 2006. These studies developed very different retrieval techniques, applied to satellite measurements from SCIAMACHY/Envisat and POLDER/PARASOL. A time series of the DRE, retrieved by both satellites, is used to compare the two. Differences in DRE retrieval resulting from limitations of the instruments and methodologies are discussed separately as technical differences. When technical differences are minimized by comparing spatial overlapping data, the agreement of both DRE results improves significantly. The mean difference in DRE ($\Delta$DRE) is reduced from 16.9 Wm$^{-2}$ to 10.3 Wm$^{-2}$ as a result of this, a reduction of 39%. Three potential causes for the remaining differences are discussed. First, SCIAMACHY underestimates the DRE by approximately 5%, which explains about 15% of the remaining overlapping $\Delta$DRE. Secondly, the POLDER DRE is based on a relatively high aerosol optical thickness (AOT), compared to other instruments and an overestimation of both the AOT and DRE is expected. Third, the effect of a thicker cloud cover during SCIAMACHY retrieval is suggested to be approximately equivalent to a systematic DRE difference between the methods. Although the methods are vastly different, the agreement in DRE retrieval is good and it is recommended to apply the SCIAMACHY method to different instruments.

# Table of contents

# 1. Introduction

The interaction between aerosols and solar radiation represents one of the largest uncertainties in our understanding of the climate. The main cause of uncertainties is the interaction of aerosols with clouds. Among other things, aerosols affect the cloud albedo, the cloud lifetime and the cloud formation by acting as cloud condensation nuclei and by changing the vertical stability of the atmosphere. The impact of aerosols on climate is not limited to these semi-direct and indirect effects. There is also the direct interaction of aerosols with radiation through scattering and absorption processes. Although this so called "direct radiative effect" (DRE) is well understood, it is currently still difficult to simulate by climate models [*Yu et al.*, 2006][*Forster et al.*, 2007].

Over a dark background, like the ocean, aerosols increase the amount of radiation backscattered to space, which increases the local planetary albedo. The net DRE of the aerosol layer at the top of the atmosphere is negative and associated with a cooling effect. However, when there is an aerosol layer over a brightly clouded area, it can decrease the amount of radiation backscattered to space, depending on the balance between scattering and absorption processes. A net positive DRE can be obtained when aerosol absorption outweighs scattering, resulting in a warming effect. The latter can be obtained when a layer of absorbing aerosols, like those from biomass burning events, is located above a heavily and brightly clouded area. It is this phenomenon that is the subject of this study.

The radiative properties of above-cloud aerosols (ACA) are often studied in the South East Atlantic, near the coast of the southern African region. This region is well suited because of the annual reoccurrence of biomass burnings during the local dry season and the nearly permanent (partial) cloud cover of marine stratiform clouds over which the light absorbing particles are advected [*De Graaf et al.*, 2012].

The aim of this paper is to analyse the DRE of ACA provided by two different methods, described by *De Graaf et al.* (2012) and *Peers et al.* (2015). Both studies have developed a unique method to retrieve the DRE of ACA using measurements from SCIAMACHY/Envisat and POLDER/PARASOL respectively. This study will focus on the data acquired from the first of June to the 30th of September of 2006 over the South East Atlantic. During August 2006 both methods detected a strong warming effect, with an average net DRE at the top of the atmosphere (TOA) of 23 Wm$^{-2}$ for SCIAMACHY retrieval and 33.5 Wm$^{-2}$ for POLDER retrieval.

While these results are in the same order of magnitude, the difference is significant. This highlights the need for a quantitative comparison in order to validate these methods. The aim of this study is to understand the difference between the DRE measured by *De Graaf et al*. (2012) and *Peers et al.* (2015) and to discuss potential causes of the differences.

The second chapter of this paper describes the data sets used in this study, both in terms of the instruments and retrieval methods. In the third chapter, the methodology used to compare the DRE will be discussed. The fourth chapter shows the results of this comparison. In the fifth chapter, we will highlight three interesting cases and explain the results and discuss the role of the technical differences. In the sixth chapter, we will investigate three possible sources of remaining differences, after the technical differences are minimized. Finally, conclusions are drawn in the seventh chapter.

# 2.  Data

This chapter describes the data used throughout this study. The instruments, the processing methods and their use throughout this study will be briefly discussed. All data used in this study is retrieved between the first of June and the 30th of September, within the area between 10° and -20° latitude and -10° and 20° longitude, which can be seen in figure 1.

## 2.1 MERIS RGB

The Medium Resolution Imaging Spectrometer (MERIS), part of the Envisat payload, is an imager with 15 channels in the solar spectral range. It provides an excellent collocation with SCanning Imaging Absorption SpectroMeter for Atmospheric CHartographY (SCIAMACHY) measurements. The RGB images were produced using MERIS Reduced Resolution Geolocated and Calibrated TOA Radiance. The images are used to visualize the (cloud) conditions at the moment of the DRE retrieval by SCIAMACHY for a single day. As an example, the MERIS true color image of the 13th of August can be found in figure 1. The large patches of white that can be seen are the areas where the instrument does not retrieve any data due to its orbit and swath width.



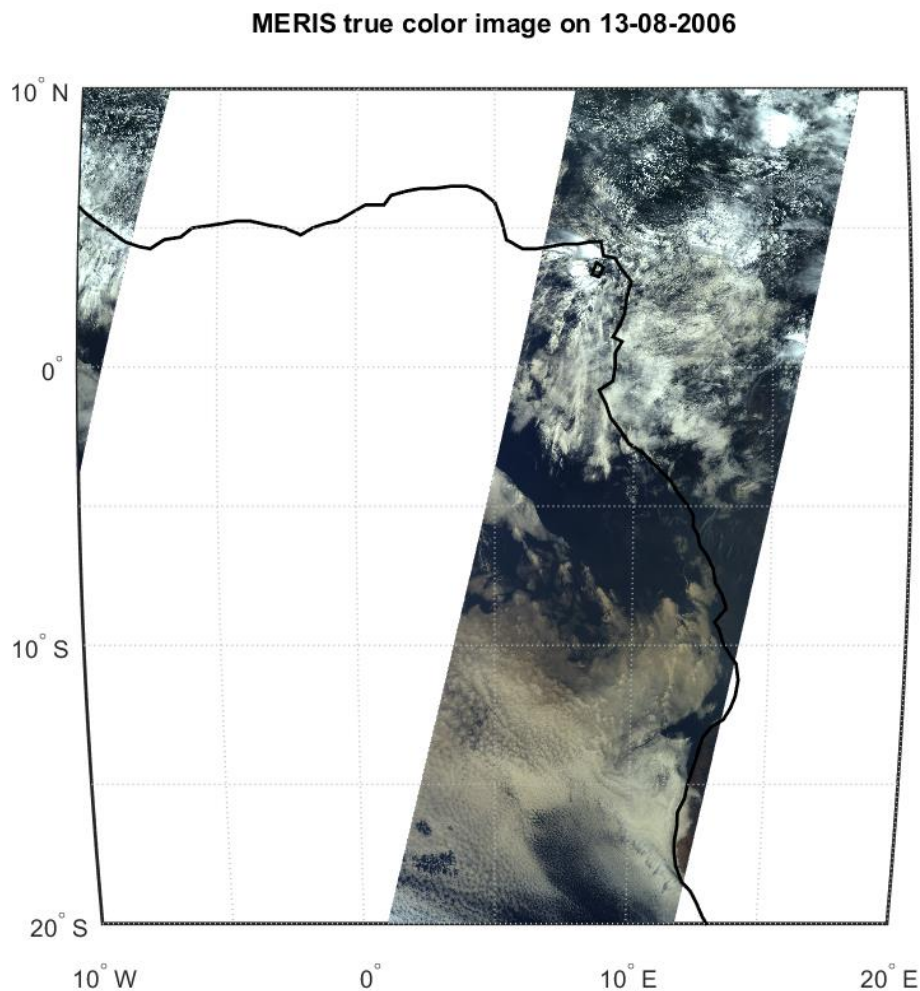MERIS true color image on 13-08-2006

**Figure 1. The cloud and smoke conditions on the 13th of August 2006, shown by MERIS RGB imagery. SCIAMACHY passes over the area of the South East Atlantic in descending orbit, from north to south, in the morning.**

## 2.2 MODIS RGB

The MODerate-resolution Imaging Spectroradiometer (MODIS), part of the Aqua payload and part of the A-train constellation, is a spectroradiometer that captures data in 36 spectral bands, ranging in wavelengths from 400 to 14400 nm at varying spatial resolutions. It is part of the A-train constellation, a satellite constellation of six Earth observation satellites in sun-synchronous orbit at an altitude of about 700 km. As part of the A-train and with a larger swath width, it provides an excellent collocation with Polarization and Directionality of the Earth's Reflectance (POLDER) measurements. The RGB images were produced using the Level 1B Calibrated Radiances at 500m and 1 km, as well as the geolocation at 1 km. The images are used to visualize the (cloud) conditions at the moment of the DRE retrieval by POLDER for a single day. Similar to RGB images from MERIS, the RGB images from MODIS aim to explain differences in the DRE retrieval of the two methods. As an example, the MODIS true color image of the 13th of August can be found in figure 2.
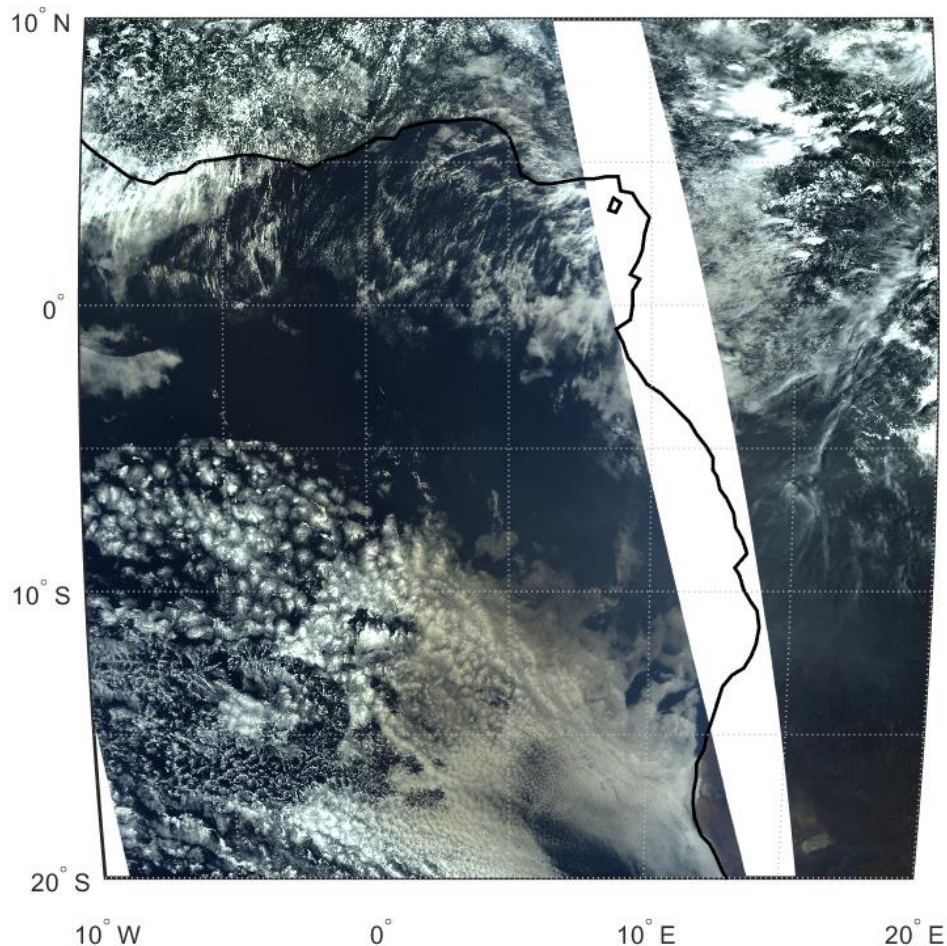


**MODIS true color image on 13-08-2006**

**Figure 2. The cloud and smoke conditions on the 13th of August 2006, shown by MODIS RGB imagery. POLDER and MODIS pass over the area of the South East Atlantic in ascending orbit, from south to north, in the early afternoon.**

## 2.3 SCIAMACHY DRE retrieval

As part of the payload of the European Space Agency's Environmental Satellite (Envisat), SCIAMACHY is an imaging spectrometer, designed to measure sunlight, transmitted, reflected and scattered by the atmosphere or surface of Earth. It measures in eight channels from 240 to 2380 nm at a spectral resolution of 0.2 – 1.5 nm. The instrument was launched on the first of March 2002 into a polar orbit at about 800 km altitude, orbiting the Earth every 100 minutes, with an equator crossing-time of 10:00 a.m. (local time) for the descending node [*Bovensmann et al.*, 1999].

SCIAMACHY measures in two alternating modes, nadir and limb. When observing the radiance in nadir mode, SCIAMACHY scans the Earth with a footprint of about 960 x 490 km$^2$ with a resolution of about 60 x 30 km$^2$. Only data from nadir mode measurements are used to calculate the DRE.

The most relevant properties for this study, retrieved from SCIAMACHY reflectance measurements, are the reflectance spectrum between 240 nm and 1750 nm, the cloud optical thickness (COT) and droplet effective radius ($r_{eff}$) of the clouds. The method of *De Graaf et al.* (2012) uses these two cloud parameters to model the unpolluted cloud spectra. This modeled reflectance is compared to the reflectance measurements from SCIAMACHY to retrieve the DRE.

The cloud properties, COT and $r_{eff}$, are retrieved from SCIAMACHY reflectance from wavelengths between 1000 nm and 2500 nm, where the reflectance carries information on both parameters [*Nakajima, T., and M. D. King,* 1990]. The Nakajima/King algorithm was adopted by *De Graaf et al.* (2012) to retrieve the cloud parameters from reflectance measurements at two wavelengths, 1246 and 1640 nm. It was assumed that retrieval at 1246 nm is unaffected by aerosols and, as a result, that the aerosol optical thickness (AOT) is zero at this wavelength.

To model the unpolluted cloud signal, a reflectance lookup table (LUT) was created of reflectances for scenes with clouds under various conditions at wavelengths outside the major gas absorption bands, for a range of cloud parameters. Only water clouds were modeled, which are the most likely ones encountered when aerosols overlie the clouds. A gamma-distribution was used for the effective radius, varying between 3 and 24 μm. The COT was varied from 2 to 48. By applying the measured cloud properties to this LUT, the aerosol-free cloud spectrum is modeled. The effect of absorption by aerosols is found by subtracting the retrieved reflectance from the modeled reflectance. From this, the DRE of the aerosols ($\Delta \mathcal{E}$) is calculated using equation 1 [*De Graaf et al.*, 2012*].

$$\Delta \mathcal{E} = \int_{240\,nm}^{1750\,nm} \frac{\mu_0 E_0 (R_{cld} - R_{cld+aer})}{B_{cld}} d\lambda + \epsilon \qquad (1)$$

In this equation, $R_{cld}$ is the reflectance of the unpolluted scene, $R_{cld+aer}$ is the reflectance of the polluted scene, $E_0$ is the downwelling solar irradiance, $\mu_0$ is the cosine of the solar zenith angle, $B_{cld}$ is the anisotropy factor and $\varepsilon$ is the error in the algorithm. The anisotropy factor is a measure for the angular distribution of the reflected radiation for a scene, which is assumed to be equal for aerosol-unpolluted and aerosol-polluted scenes.

Retrieving aerosol properties in cloudy skies is especially challenging. Therefore, not making assumptions on aerosol properties is a major advantage of this method. To ensure the retrieval of the positive DRE, retrieval conditions were set up regarding the measurements. Only measurements of scenes with a cloud fraction (CF) higher than 0.3 are considered, all other measurements were discarded. The CF is retrieved using the FRESCO algorithm [*Wang et al.*, 2008].

The main uncertainties of the SCIAMACHY DRE retrieval method result from residual AOT and errors in the modeled aerosol-free cloud spectrum. The uncertainty of the pixel-to-pixel measurements of the aerosol DRE of this method is 8 Wm$^{-2}$ [*De Graaf et al.*, 2012].

As an example, the DRE retrieval on the 13th of August, where an exceptionally high AOT can be found in the region, is shown in figure 3. This day has been described many times, e.g. *De Graaf et al.* (2012), *Peers et al.* (2015) and *Jethva et al.* (2013). The colors in figure 3 indicate the amount of DRE that is retrieved. The scale of the colorbar is set to be the same for both SCIAMACHY and POLDER retrieval, with blue being the lowest (0 Wm$^{-2}$ or even slightly negative DRE) and red being the highest (300 Wm$^{-2}$ or higher). The image clearly shows the low resolution of SCIAMACHY as well as the ground track of SCIAMACHY. It can be seen that SCIAMACHY only retrieves the DRE over ocean clouds. The gaps between the measurements are a result of the two alternating modes.
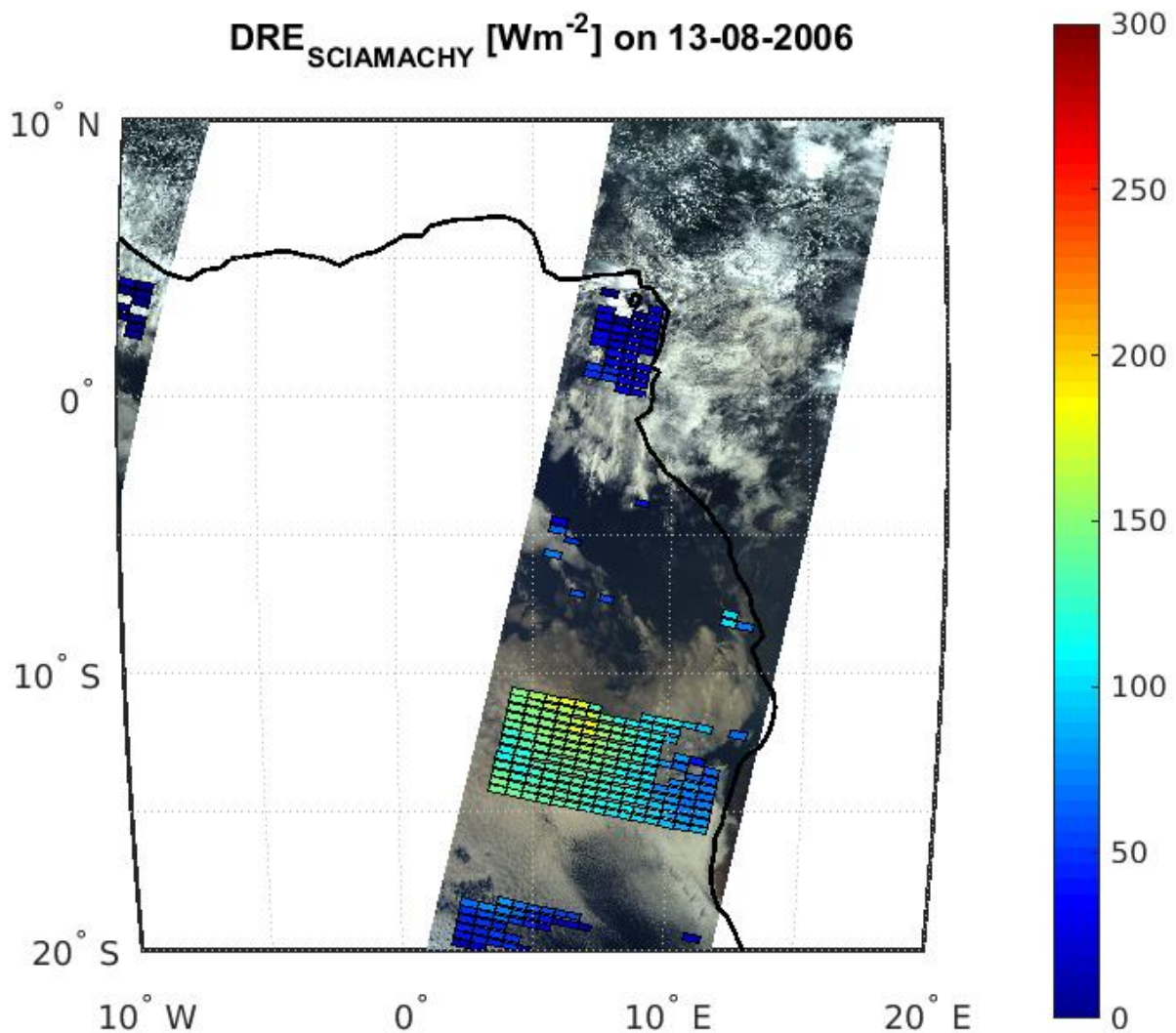


Figure 3. The cloud and smoke conditions on the 13th of August 2006, shown by MERIS RGB imagery, overlaid with SCIAMACHY DRE retrieval. SCIAMACHY passes over the area of the South East Atlantic in descending orbit, from north to south, in the morning.

## 2.4 POLDER DRE retrieval

The POLDER instrument, the main part of the PARASOL (Polarization and Anisotropy of Reflectances for Atmospheric Science coupled with Observations from a Lidar) satellite's payload, is a passive optical imaging radiometer and polarimeter. The satellite was launched on the 18th of December 2004. For five years, it was part of the A-train constellation. The instrument provides radiances for nine spectral bands between 443 and 1020 nm in addition to polarization measurements over three spectral bands (i.e. 490, 670 and 865 nm), with a ground spatial resolution of 5.3 x 6.2 km$^2$ and swath width of about 1100 km [*Deschamps et al.*, 1994]. All measurements of POLDER are projected on a fixed global reference grid.

The distinctive feature of the POLDER DRE retrieval method by Peers et al (2015) is to combine information from polarization measurements with total radiance measurements. Polarization radiance measurements allow for the retrieval of the scattering AOT and the aerosol size distribution. There are two effects of aerosols on polarization. The first one is to attenuate the large peak of the signal around a scattering angle of 140°, caused by the liquid cloud droplets. The second effect is to create an additional signal at side scattering angles. The effect of absorption is assumed to be very weak at these angles; therefore this signal is mostly a result of the scattering processes of aerosols.

These aerosol properties, together with the total radiance measurements, are used to determine the absorption by the aerosol layer, as well as the COT. Using this method, the retrieval of the aerosol properties is done with minimal assumptions and with the cloud properties corrected from the aerosol absorption. This DRE retrieval method also applies retrieval conditions to the measurements to ensure retrieval of positive DRE. The DRE is only calculated for measurements where the geometric CF is one and the COT is larger than 3.0, all other data were discarded. The latter restriction was set because polarization measurements are independent of COT for values larger than 3.0.

Using the retrieved aerosol and cloud properties (i.e AOT, aerosol size distribution and COT), the DRE is processed by simulating the fluxes (with and without aerosol) with a radiative transfer code. The retrieved DRE on the 13th of August 2006 is shown in figure 4 as an example. The colorbar of this figure is the same as in figure 3, which allows for easy comparison. The figure shows the high resolution of POLDER, as well as the ground track of the satellite, which both differ strongly from SCIAMACHY. POLDER also retrieves the DRE only over brightly clouded scenes which fit the retrieval conditions.
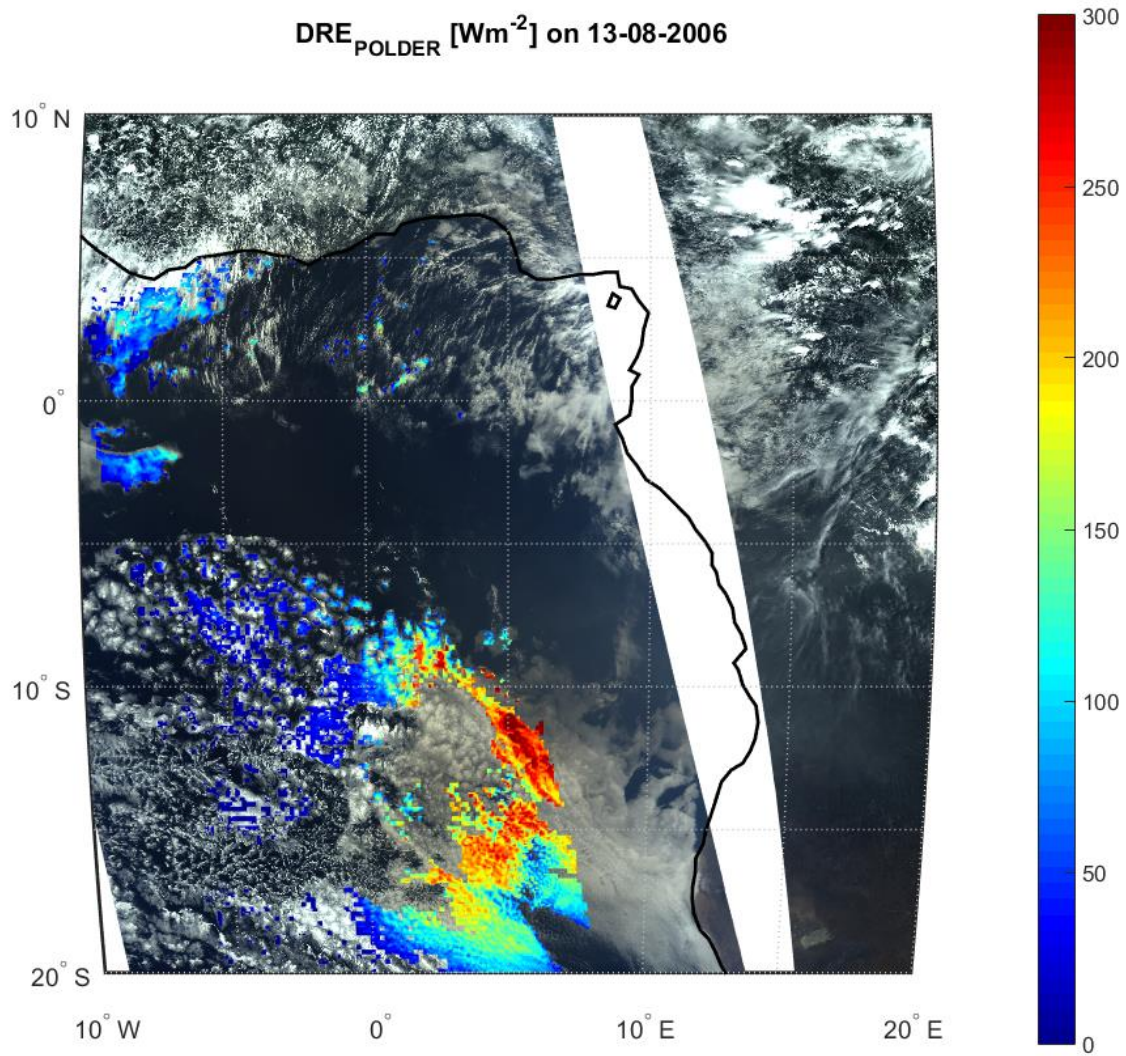
**Figure 4. The cloud and smoke conditions on the 13th of August 2006, shown by MODIS RGB imagery, overlaid with POLDER DRE retrieval. POLDER and MODIS pass over the area of the South East Atlantic in ascending orbit, from south to north, in the early afternoon.**

# 3. Methodology

This section describes the methodology that was used to compare the DRE retrieval from SCIAMACHY and POLDER. This chapter discusses seven subjects:

1. Outliers in the DRE data sets
2. Differences in solar zenith angle (SZA)
3. The use of single day retrieval
4. The calculation of the regional median DRE
5. Technical differences, the concept and minimization
6. Aerosol optical thickness
7. Cloud optical thickness

## 3.1 Outliers

The provided results of the DRE retrieval by SCIAMACHY contain errors. Some errors result in outliers, ranging between -5.000 Wm$^{-2}$ and 22.000 Wm$^{-2}$. These outliers can easily be seen in the histogram of figure 5, containing all DRE retrievals of both SCIAMACHY (figure 5a) and POLDER (figure 5b), from the first of June until the 30$^{th}$ of September. These outliers are removed by removing all data outside of arbitrary boundaries in which most of the data will be preserved.
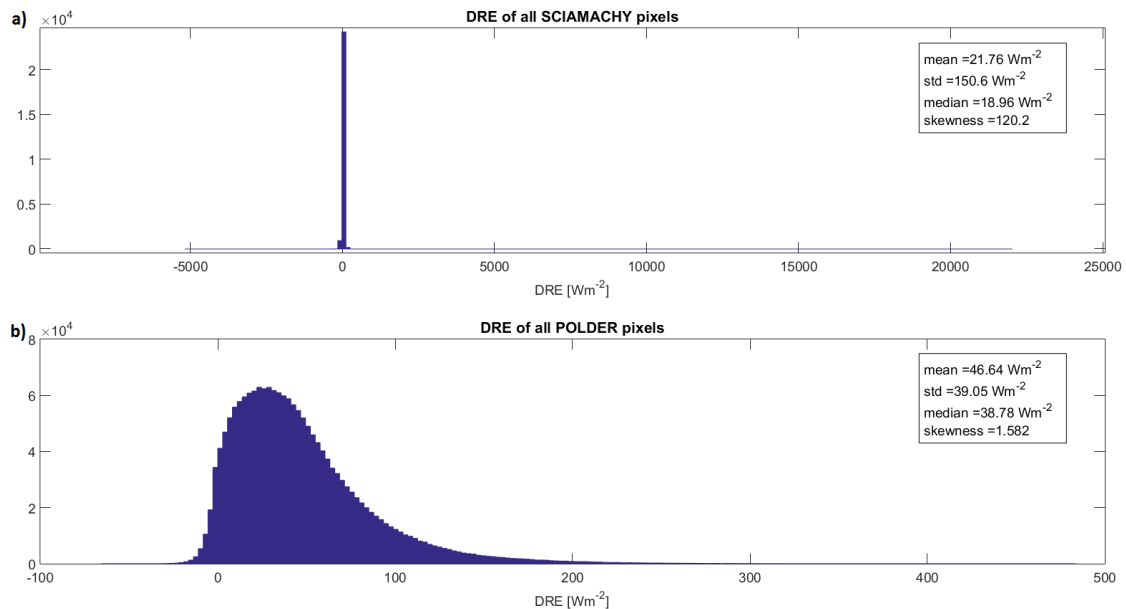


**Figure 5. (a) A histogram of the DRE without boundaries, retrieved with SCIAMACHY from the first of June until the 30$^{th}$ of September 2006 over the South East Atlantic. A large peak is visible around 0 DRE as a result of large outliers ranging from -5000 Wm$^{-2}$ to 22000 Wm$^{-2}$. (b) A histogram of the DRE without boundaries, retrieved with POLDER from the first of June until the 30$^{th}$ of September 2006 over the South East Atlantic.**

The outliers result from errors in the modeled reflectance spectrum of the unpolluted cloud scene. As a result of interpolation errors in the LUT used to model the unpolluted scene, the provided DRE data set contains errors. The errors in the lookup table interpolation do not occur often, only at the edges of the parameter space. Most often, the errors occur with high effective droplet radii. Smaller errors can often be found at an effective droplet radius close to 20 μm and the large outliers are

found when the effective droplet radius is significantly higher than 20 μm, while the limit of the LUT is 24 μm.

These errors range from a few Watts per square meter to sometimes over a thousand Watts per square meter, both positively and negatively. Very large errors are detected as outliers, but the smaller errors of just a few Watts are very difficult to detect. Even though they are small, they have a significant effect when calculating the mean of the DRE measurements. In order to minimize the impact of the lookup table errors, the DRE results of POLDER and SCIAMACHY are studied by comparing the regional median DRE.

The boundaries result from studying the histograms of all DRE data of both SCIAMACHY and POLDER. Most of the retrieved DRE by SCIAMACHY ranges between -50 Wm$^{-2}$ and 150 Wm$^{-2}$, as shown in the histograms of figure 6. The POLDER histograms of figure 5b and figure 6b indicate that DRE retrieval higher than 150 Wm$^{-2}$ is possible. With that in mind, the boundaries are set to - 150 Wm$^{-2}$ and 350 Wm$^{-2}$ for SCIAMACHY DRE retrievals. As a result, 0.16% of the SCIAMACHY data is discarded.
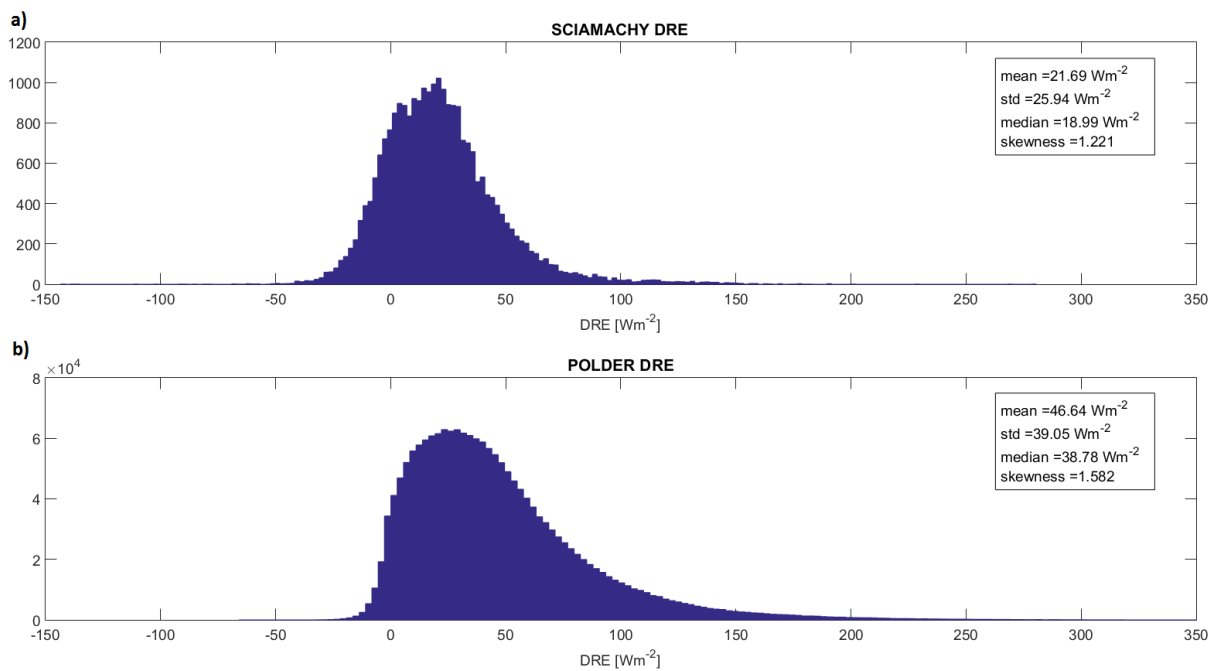


Figure 6. (a) A histogram of the DRE within the boundaries of -150 Wm$^{-2}$ and 350 Wm$^{-2}$, retrieved with SCIAMACHY from the first of June until the 30$^{th}$ of September 2006 over the South East Atlantic. (b) A histogram of the DRE within the boundaries of -150 Wm$^{-2}$ and 350 Wm$^{-2}$, retrieved with POLDER from the first of June until the 30$^{th}$ of September 2006 over the South East Atlantic. Setting these boundaries removes outliers while preserving the relevant data.

## 3.2 Solar zenith angle

The difference in overpass time between the SCIAMACHY and POLDER instruments results in a difference in the SZA at which the reflectance measurements are taken. The DRE retrieval of both data sets will be converted to nadir direction by using equation 2, where $\theta_s$ is the SZA, DRE is the DRE in nadir direction and DRE$_{SZA}$ is the DRE retrieved by SCIAMACHY or POLDER. All further DRE results that are shown in this study are converted to nadir direction.

$$DRE = DRE_{SZA}/\cos(\theta_s) \qquad (2)$$

## 3.3 Single day DRE retrieval

When comparing the DRE retrieval of SCIAMACHY and POLDER, three days of measurements with distinct features will be highlighted. These so called "single day DRE retrieval images" will show the retrieved DRE by the two methods, as well as the corresponding RGB images. The goal of these images is to visualize both the effect of the difference in orbit and key differences in DRE retrieval between the two methods. Examples can be found in figures 3 and 4.

## 3.4 Regional median

For each day in both the SCIAMACHY and POLDER data set, the regional median DRE is calculated as well as the difference between the two regional median values, ΔDRE. The regional median is the median value over all measurements in the whole region. In this study, the Δ refers to the difference between the data of SCIAMACHY and POLDER, described by equation 3, where *x* can be any parameter. The three resulting DRE median values are displayed as a time series in order to compare the retrieved DRE of both methods and to identify the differences.

$$\Delta x = x_{POLDER} - x_{SCIAMACHY} \qquad (3)$$

## 3.5 Technical differences

### The concept

There are many reasons for why the retrieved DRE by SCIAMACHY and POLDER is different. Some of these reasons can be traced back to the limitations of the instruments that were used. These differences in limitations cause a significant part of the difference in DRE between SCIAMACHY and POLDER. However, their effect can be minimized and it is for that reason that they are discussed separately in this study as technical differences.

When discussing technical differences, the method by which the DRE is retrieved from the measurements is not taken into account. Major causes of technical differences are: the difference in resolution (about 60 x 30 $km^2$ and 6 x 6 $km^{-2}$ for SCIAMACHY and POLDER respectively), the different swath widths (490 km and 1100 km), the different satellite tracks, the difference in overpass time (about 3.5 hours) and the difference in retrieval conditions. The large gaps along the track in between the SCIAMACHY retrieval are also a cause of technical differences and result from the instrument measuring in limb mode, which is not suited for DRE retrieval. It is important to note that the retrieval conditions of both methods cannot be compared. The CF resulting from the FRESCO algorithm cannot be compared to the geometric CF that is used for POLDER with the available data.

The technical differences cause two major problems for the comparison: the two instruments retrieve the DRE at different locations and at different times. The first problem, the different locations, results from differences in resolution, swath width, ground tracks and retrieval conditions. The second problem, the time difference, is caused by the difference in overpass time. Even though the difference is only about 3.5 hours, it can result in large changes in the structure of the clouds. The effect of the time difference is assumed to be small on the aerosols, but not on the clouds.
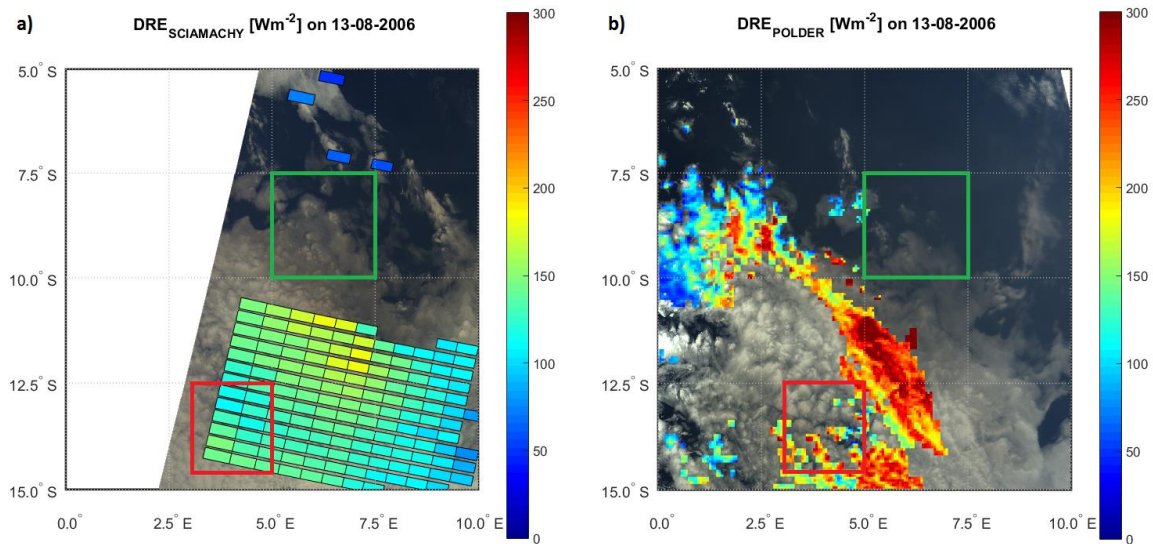
**Figure 7. (a)** The cloud and smoke conditions on the 13th of August 2006, shown by MERIS RGB imagery, overlaid with SCIAMACHY DRE retrieval, for the region constraint between -5° and -15° latitude and 0° and 10° longitude. The green square highlights an area with significant cloud cover. The red rectangle highlights that SCIAMACHY does retrieve DRE in this area. **(b)** The cloud and smoke conditions on the 13th of August 2006, shown by MODIS RGB imagery, overlaid with POLDER DRE retrieval, for the region constraint between -5° and -15° latitude and 0° and 10° longitude. The time difference between retrievals is about 3.5 hours. The green square highlight an area where the clouds have mostly dissolved in this time. The red rectangle highlights that POLDER hardly retrieves DRE in this area as a result of the retrieval conditions of the POLDER method.

The effect of the technical differences is visualized in figure 7, where the DRE from SCIAMACHY and POLDER are shown in figure 7a and 7b respectively. The two images of figure 7 are the same as figure 4 and 5, but the area is limited between -5° and -15° latitude and 0° and 10° longitude in this figure.

The difference in resolution is clearly visible in figure 7 and causes the retrieved DRE from SCIAMACHY to be averaged over a much larger area compared to POLDER. As a result of a different ground track, SCIAMACHY does not retrieve anything between 0° and 2.5° longitude, while POLDER does. The effect of the difference in retrieval conditions is visible in the area highlighted with the red rectangles, where SCIAMACHY does retrieve DRE and POLDER mostly does not. The above mentioned effects of the technical differences will be minimized, which is discussed in the next section.

The effect of the final cause of technical differences, the different overpass times, can be seen in the area highlighted by the green squares in figure 7. In this area, most of the clouds visible in figure 7a have dissolved in figure 7b, when POLDER passes over the area. The effect of this change in cloud structure is very complex and can be the subject of a new study by itself. Therefore, this effect will not be studied in this report and its effect will not be minimized like the other technical differences. However, it will be taken into account when analyzing the results of this comparison study.

Technical differences play a large role in the comparison of the DRE retrieval by SCIAMACHY and POLDER, but there will still be a discrepancy in the DRE of both instruments after minimization. When two instruments retrieve the same properties, the results are always (at least slightly) different, as can be seen in the comparison study of the AOT by *Jethva et al.* (2013) for example. Once the technical differences are minimized, it is expected that there will still be a difference in DRE. The remaining differences will be studied by discussing three likely causes of the DRE difference in chapter 6. The changes in cloud structure are taken into account, but will not specifically be discussed.

## Minimizing technical differences

In order to study the impact, the regional median for pixels with spatially overlap is calculated for each day. Spatial overlap is defined by the center coordinates of a certain number of POLDER pixels that must be located within a SCIAMACHY pixel. The percentage of overlap is calculated by taking the number of retrieved POLDER DRE pixels overlapping with a SCIAMACHY DRE pixel, and dividing it by the number of POLDER reference grid pixels that lie within said SCIAMACHY pixel.

In order to define the necessary conditions to calculate the overlapping regional median DRE, two parameters are used. The first condition, $C_{overlap}$, determines the minimum percentage of each SCIAMACHY pixels that needs to be filled with POLDER pixels. The second condition, $C_{min}$, determines the minimum number of overlapping SCIAMACHY pixels needed to calculate the regional median. The latter condition is used to assure the statistical significance of the regional median. Data that does not meet one of these conditions is discarded.
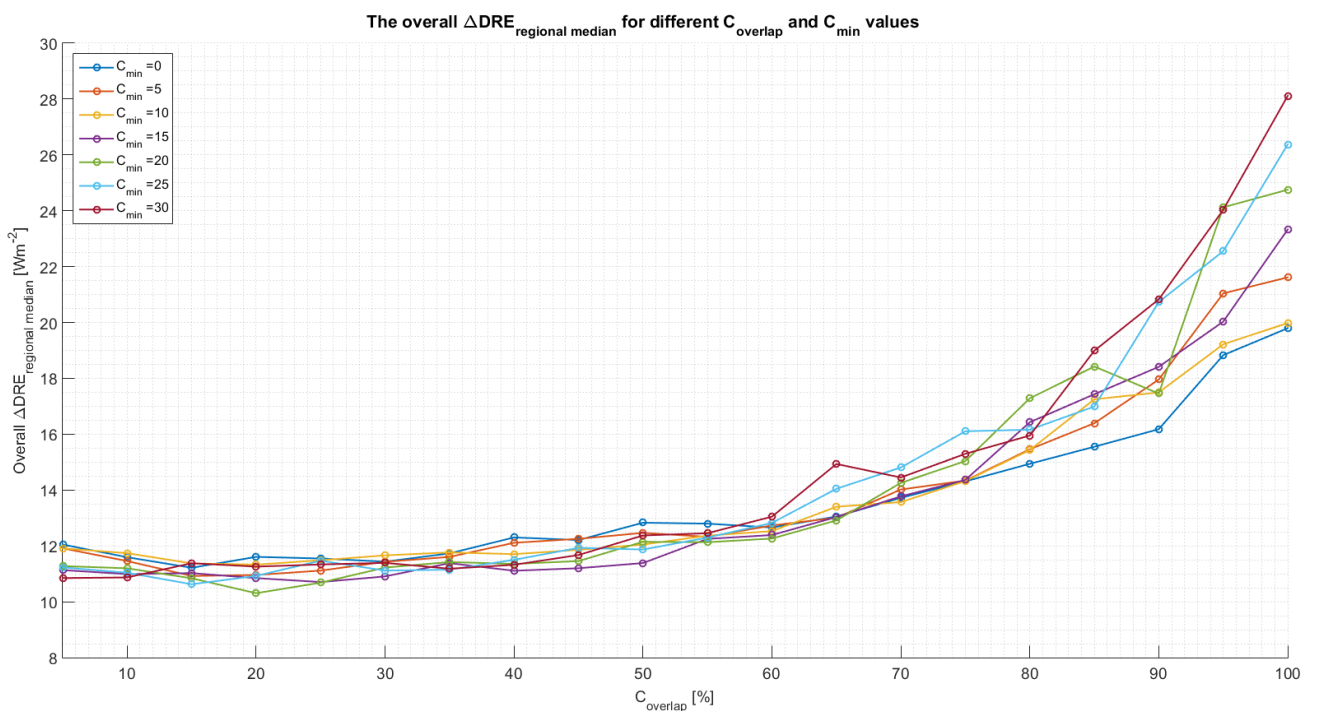


**Figure 8. The overall ΔDRE_regional median as a function of condition $C_{overlap}$ (on the x-axis) for several $C_{min}$ (in different colors). $C_{overlap}$ determines the minimum percentage of the larger SCIAMACHY pixel filled by smaller POLDER pixels, before the pixels are considered to overlap. A significant reduction in overall ΔDRE_regional median can be found for all values of $C_{min}$ between 5% and 50% for $C_{overlap}$. The overall ΔDRE_regional median shows strong agreement for values of $C_{min}$ between 0% and 60% for $C_{overlap}$. The smallest overall ΔDRE_regional median is found for $C_{overlap}$ = 20% and $C_{min}$ = 20.**

In order to find the definitive values for the $C_{overlap}$ and $C_{min}$, the effect of these conditions on the mean of the regional median ΔDRE over all days, the overall ΔDRE_regional median, is studied. The overall ΔDRE_regional median is calculated for each condition. The result is shown in figure 8, where $C_{overlap}$ is on the x-axis, the overall ΔDRE_regional median is on the y-axis and $C_{min}$ is shown in different colors.

A significant reduction in overall ΔDRE_regional median is found for all values of $C_{min}$ as a result of small percentages of overlap, which is displayed in figure 8. The overall ΔDRE_regional median is lowest between 5% and 50% overlap for all values of $C_{min}$. The effect of $C_{min}$ is small between 5% and 50% overlap, with a biggest change in overall ΔDRE_regional median of about 1.5 Wm$^{-2}$. All conditions between 5% and 50% overlap are suitable choices for $C_{overlap}$ and $C_{min}$. As a result, the conditions that are used in this

15

study to calculate overlap are subjective. For this study, values of 20% and 20 for $C_{overlap}$ and $C_{min}$ respectively are chosen because it results in the smallest total $\Delta DRE_{regional\ median}$.

The effect of the two conditions is small between a $C_{overlap}$ of 5% and roughly 60%. For values of $C_{overlap}$ larger than 60%, the total $\Delta DRE_{regional\ median}$ shows significant increase and also the effect of $C_{min}$ increases, as can be seen in figure 8. For $C_{overlap}$ larger than about 60%, the amount of data remaining is too low and only a few days and a relatively small area is used for comparison each day. As a result, other aspects, like changes in cloud structure, become dominant.

The percentage of remaining data that remains when a $C_{overlap}$ of 20% is considered is about 25% and about 10% of the available data of SCIAMACHY and POLDER respectively. All other data are discarded when calculating the regional median DRE and regional mean values of other properties. These percentages are reduced with increasing $C_{overlap}$ and are hardly affected by $C_{min}$. This difference between the two instruments is a result of the difference in resolution and swath width. This effect is shown in figure 9 for different combinations of $C_{overlap}$ and $C_{min}$.
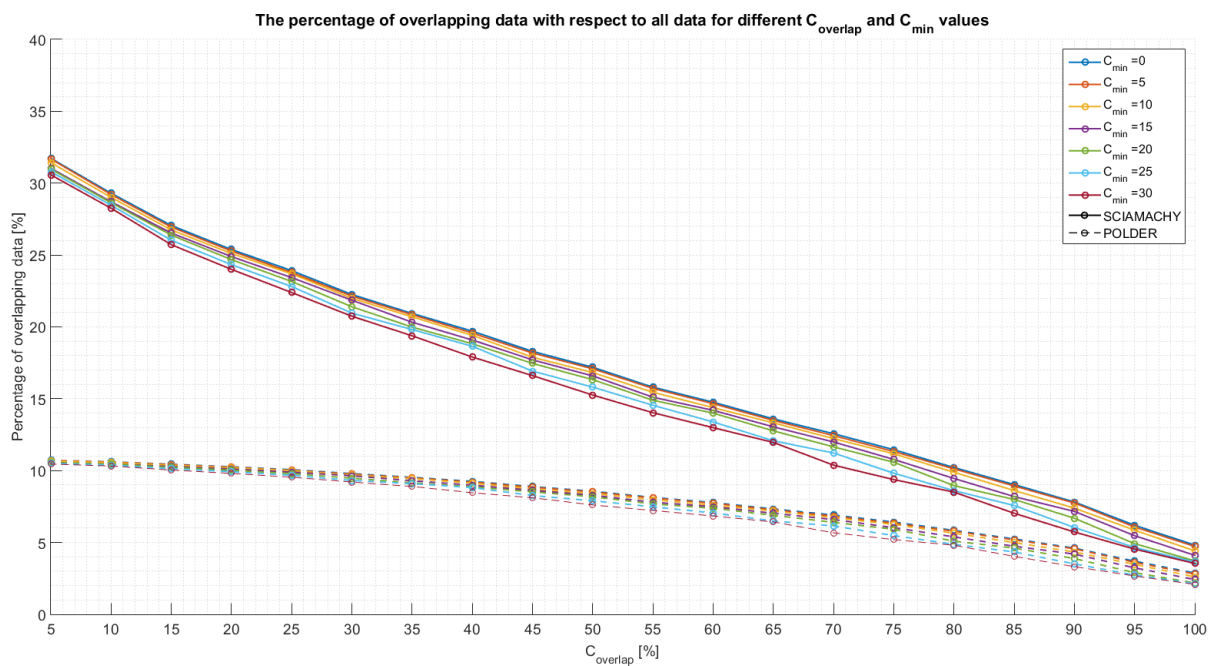


**Figure 9. The percentage of data remaining for SCIAMACHY (solid lines) and POLDER DRE (dotted lines), depending on $C_{overlap}$ (on the x-axis) and $C_{min}$ (in different colors). When only considering overlapping data, less than 32% of all SCIAMACHY data and less than 11% of all POLDER data is used. This percentage reduces with increasing $C_{overlap}$ but is hardly affected by $C_{min}$.**

As shown in figure 9, the amount of overlapping data that is available for SCIAMACHY is significantly smaller than the available POLDER data. A histogram of all overlapping data can be found in figure 10 for retrieval by both SCIAMACHY (figure 10a) and POLDER (figure 10b), with the relevant statistics. The satellites retrieve a median DRE of 27.93 Wm$^{-2}$ and 39.45 Wm$^{-2}$ for SCIAMACHY and POLDER respectively, for full region and time period. Both distributions peak around 25 Wm$^{-2}$, but POLDER has more high positive DRE retrievals, which is reflected by a higher mean, median and skewness. This is most likely a result of the higher resolution of POLDER. The large resolution of SCIAMACHY causes the retrieved DRE to be averaged over a much larger area. As a result, peak values will be higher for POLDER than for SCIAMACHY.
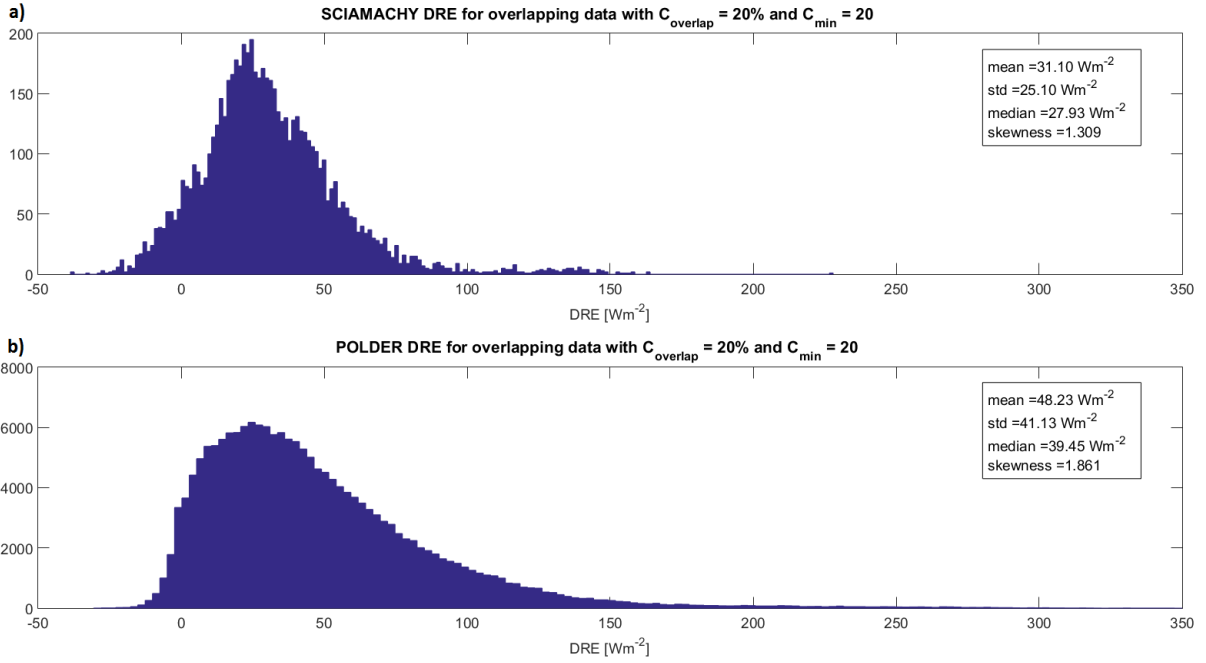
**Figure 10. (a) A histogram of all overlapping DRE data, retrieved by SCIAMACHY. (b) A histogram of all overlapping DRE data, retrieved by POLDER. The overlap is determined with conditions $C_{overlap}$ of 20% and $C_{min}$ of 20. As a result of the difference in resolution, there is significantly less data available for SCIAMACHY compared to POLDER, but both satellites retrieve the most data close to 25 $Wm^{-2}$. POLDER has more positive DRE retrieval, which is reflected in the statistics.**

## 3.6 Aerosol optical thickness

The AOT is one of the main parameters that affect the DRE. It is a measure of the extinction of the incoming solar radiation by the aerosol layer, by either absorption and/or scattering. High AOT is expected to be associated with high DRE over clouds.

As is mentioned in the section 2.4, the AOT is received with POLDER, but not with SCIAMACHY. It is dependent on wavelength and is retrieved with POLDER at multiple wavelengths, including 670 nm and 865 nm. By measuring the AOT at two wavelengths, the dependency of the AOT on wavelength can be described using the Ångström exponent ($\alpha$). By using the retrieved AOT ($\tau$) and their respective wavelengths, this exponent is calculated using in equation 4. The AOT at 550 nm and the Ångström exponent were available from the study by *Peers et al.* (2015) for this comparison study. The Ångström exponent is assumed here to be constant and can be used to convert the AOT to other wavelengths.

$$\alpha = \frac{\log(\tau_{670\,nm}/\tau_{865\,nm})}{\log(670/865)} \qquad (4)$$

SCIAMACHY does not retrieve the AOT, but it does make the assumption that it is negligible at a wavelength of 1246 nm. This assumption is challenged in section 6.1, where this assumption is expected to be a likely cause of the difference in DRE. To challenge this assumption, the AOT is converted from the available AOT at 550 nm to 1246 nm. The conversion is done using Ångström relation, shown in equation 5, which uses the AOT ($\tau$) at 550 nm and the wavelengths ($\lambda$) of 550 nm and 1246 nm.

$$\tau_{1246nm} = \tau_{550nm} \cdot \left(\frac{\lambda_{1246nm}}{\lambda_{550nm}}\right)^{-\alpha} \qquad (5)$$

A histogram of the available overlapping AOT is shown in figure 11. Using the POLDER AOT at 550 nm, the regional mean AOT is calculated using the same method as the regional median DRE. This time, the regional mean is calculated because the AOT dataset did not contain outliers, in contrast to the SCIAMACHY DRE dataset. The regional mean AOT will be used to understand the conditions under which the DRE of POLDER and SCIAMACHY is retrieved. Contrary to clouds, the aerosol layer is assumed to not have a diurnal cycle and to be mostly affected by advection. It is therefore assumed that changes in AOT as a result of the difference in overpass time are negligible.
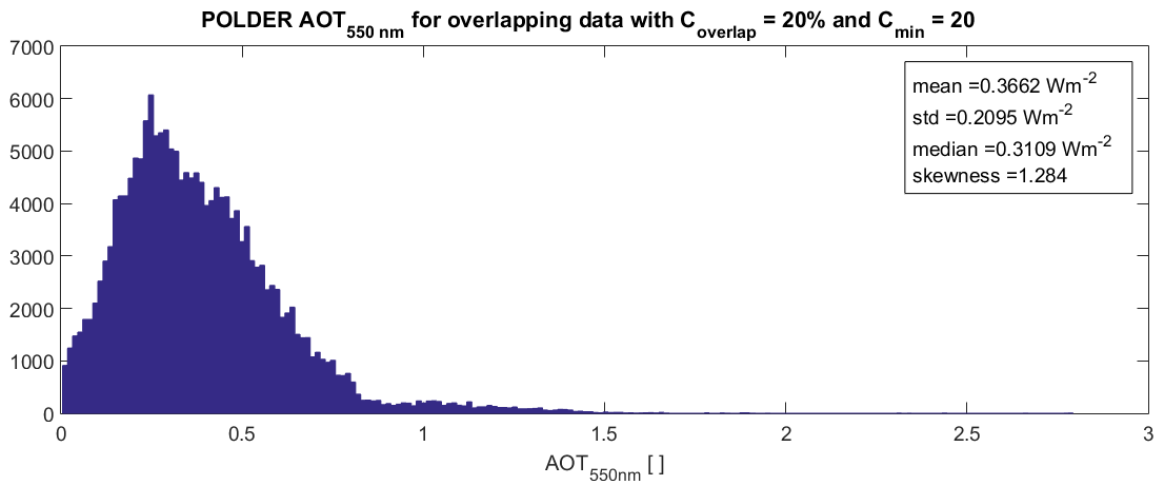


**Figure 11. A histogram of all overlapping AOT data at a wavelength of 550 nm. The overlap is determined with $C_{overlap}$ of 20% and $C_{min}$ of 20. Most of the retrieved AOT is found between 0 and 0.75, with a peak close to 0.3. A long but low tail of high AOT retrieval can be seen between 0.75 and 1.5, with some values reaching values up to 2.8.**

## 3.7 Cloud optical thickness

The COT is the other main parameter that affects the DRE. The DRE does not only depend on the aerosol layer, but it depends strongly on brightness of the background. The COT is a measure of the brightness of the clouds, which is the background over which the DRE is retrieved. The DRE can be explained as a change in brightness of said background. If the aerosol layer reduces the brightness of the background, the DRE is positive and vice versa. For similar AOT values, a brighter background, i.e. higher COT, will result in higher DRE.

The COT is retrieved by both SCIAMACHY and POLDER, as is mentioned in sections 2.4 and 2.5. SCIAMACHY retrieves cloud properties at two bands: 1246 and 1640 nm. POLDER retrieves COT from total radiance measurements, taking into account the aerosol contribution to the signal. The retrieval by POLDER is restricted to COT > 3 and COT < 42, where all retrieval of COT > 42 is set to 42. A histogram of the overlapping COT for both instruments is shown in figure 12, which clearly shows the restrictions to the POLDER COT retrieval. The spikes that are visible in the POLDER COT of figure 12b are a result of discrete sampling of the LUT, done to retrieve the COT from POLDER measurements.

Both methods of COT retrieval are very different and a comparison of the results is worth studying separately. Due to time restrictions, this will not be done in this comparison study of the DRE. Similar to the AOT, the COT is used to understand the conditions under which the DRE is retrieved. For both instruments, the regional median COT is calculated using the same method as the regional median DRE. The regional median is used for the COT instead of the regional mean, because of the restrictions that are placed on POLDER COT retrieval corrupts the mean.
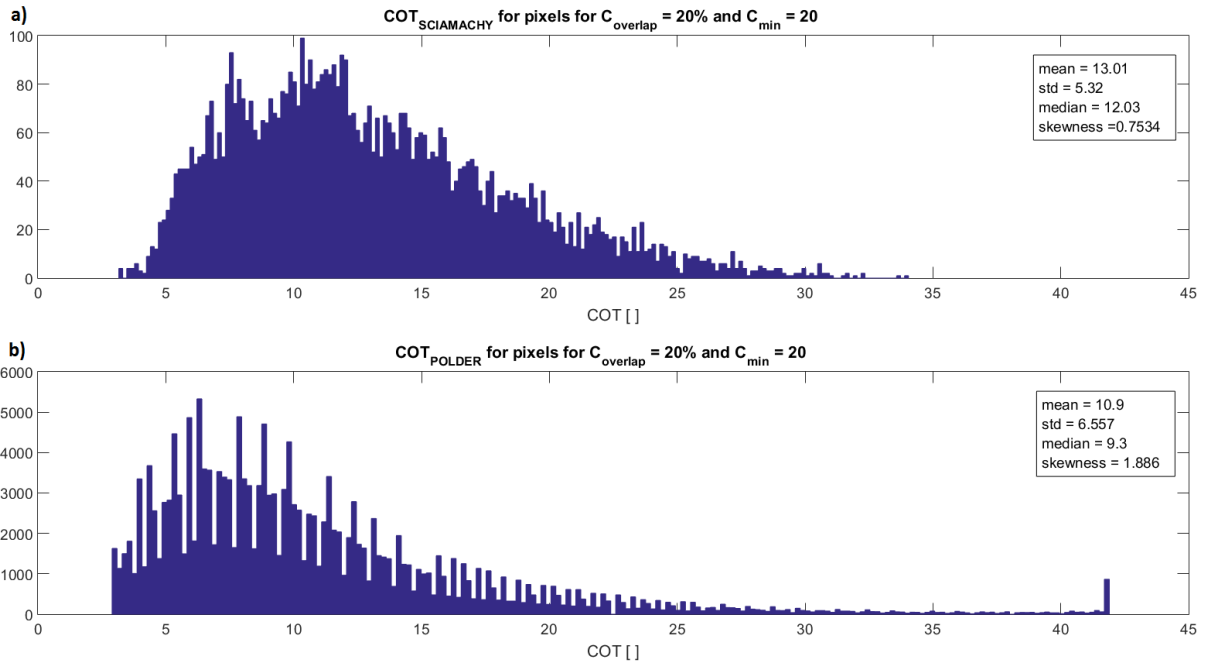
**a)**

COT$_{SCIAMACHY}$ for pixels for C$_{overlap}$ = 20% and C$_{min}$ = 20

mean = 13.01
std = 5.32
median = 12.03
skewness =0.7534

**b)**

COT$_{POLDER}$ for pixels for C$_{overlap}$ = 20% and C$_{min}$ = 20

mean = 10.9
std = 6.557
median = 9.3
skewness = 1.886

**Figure 12. (a) A histogram of all overlapping COT data, retireved by SCIAMACHY. (b) A histogram of all overlapping COT data, retrieved by POLDER. POLDER does not retrieve COT < 3 and all retrieval higher than 42 is set to 42 as a result of the boundaries of the LUT used for COT retrieval. The spikes that are visible in the POLDER COT are a result of discrete sampling of the LUT, done to retrieve the COT from POLDER measurements. The overlap is determined with conditions C$_{overlap}$ of 20% and C$_{min}$ of 20. As a result of the difference in resolution, there is significantly less data available for SCIAMACHY compared to POLDER.**

# 4. Results

## 4.1 Minimization of technical differences

The term technical differences was defined in section 3.5 as DRE differences, caused by limitations of the instruments or retrieval method. This distinction was made because the largest contributions to the technical differences can be minimized by only considering spatial overlapping data. By comparing the regional median DRE of overlapping data with the regional median DRE of all data, the effect of the technical differences can be determined. The remaining DRE difference will be discussed in chapter 6.

A time series of the regional median DRE is made for both overlapping DRE retrieval (figure 13b) and all DRE retrieval (figure 13a). In figure 13, SCIAMACHY retrieval is shown in blue, POLDER retrieval is shown in red and the difference between the two, $\Delta DRE_{regional\ median}$, is shown as a dotted black line. The mean DRE displayed in this figure is the mean over all regional median DRE values of the full time series. Note that by only retrieving the DRE of above cloud aerosols, only positive DRE is expected, as is explained in the chapter 1.

For all data, POLDER retrieves higher positive DRE compared to the SCIAMACHY retrieval, with mean regional medians of 34.5 $Wm^{-2}$ and 17.8 $Wm^{-2}$ respectively. The mean difference in regional median DRE, mean $\Delta DRE_{regional\ median}$, between the two methods is 16.9 $Wm^{-2}$. Even though the difference in $\Delta DRE_{regional\ median}$ is significant, there is agreement between SCIAMACHY and POLDER for days associated with high positive DRE, as can be seen in figure 13a.

When only overlapping data are considered (figure 13b), there is a decrease in the number of days for which the regional median is calculated. This is especially visible in June, where only 3 days of DRE retrieval match the set conditions, $C_{overlap}$ and $C_{min}$. Overall, the mean regional median DRE has increased for both SCIAMACHY and POLDER, with an overlapping mean regional median of 31.35 $Wm^{-2}$ and 42.65 $Wm^{-2}$ respectively. The agreement between SCIAMACHY and POLDER for days associated with high positive DRE has improved significantly. This is reflected in the mean $\Delta DRE_{regional\ median}$, which is reduced from 16.9 $Wm^{-2}$ to 10.3 $Wm^{-2}$. The effect of the technical differences is therefore estimated to be 6.6 $Wm^{-2}$, or 39% of the mean $\Delta DRE_{regional\ median}$ for all data. From this moment, only overlapping data will be considered, unless stated otherwise.

A very high positive DRE event is found in the middle of August. On the day before the large peak, on the 11th of August, both methods retrieve a very low DRE. The next few days, the retrieved DRE is very high, with a maximum on the 13th of August of 130.0 $Wm^{-2}$ and 174.7 $Wm^{-2}$ for overlapping SCIAMACHY and POLDER data respectively. Both SCIAMACHY and POLDER retrieve the highest DRE, but also the largest $\Delta DRE_{regional\ median}$ during this event. This event has been discussed by several people (e.g. *De Graaf et al.* (2012), *Jethva et al.* (2013) and *Peers et al.* (2015)) and the 11th and 13th of August will be used as case studies in chapter 5, as well as the 19th of August.
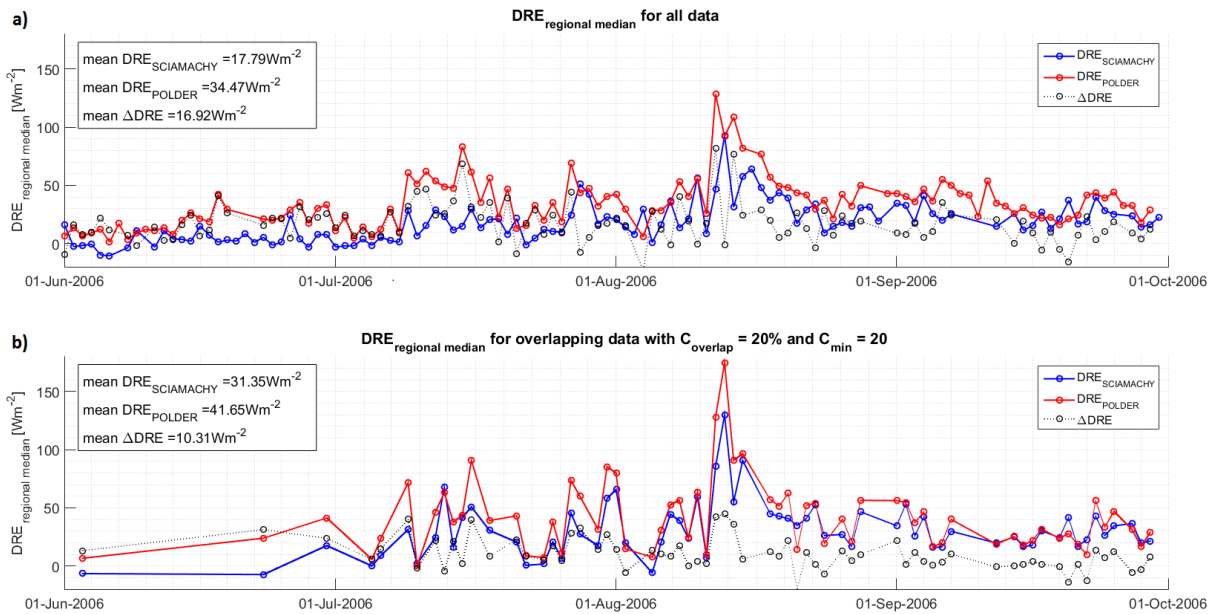
**Figure 13. A time series of the median DRE for each day, for the DRE retrieved by SCIAMACHY (blue), POLDER (red) and ΔDRE_regional median (dotted black). The time series is made for all available data (a) and for all overlapping data (b) that. The overlap is determined with conditions C_overlap of 20% and C_min of 20. The regional median is calculated by taking the median DRE for each day. The ΔDRE_regional median is the SCIAMACHY regional median DRE subtracted from the POLDER regional median DRE. The mean DRE is the total mean taken over all the regional median DRE values. Considering only overlapping data reduces the amount of days over which the regional median is calculated and reduces the mean ΔDRE_regional median by 6.61 Wm^{-2}, a reduction of about 39% which is only a result of minimizing technical differences.**

The ΔDRE_regional median is largest on days where the retrieved regional median DRE is high, as can be seen in figure 13b. The same relation can be seen in a scatterplot of the regional median POLDER DRE against the ΔDRE_regional median, shown in figure 14. Each day over which the overlapping regional median DRE is calculated is represented with a blue dot. The red line shows a least squares linear fit to the data.
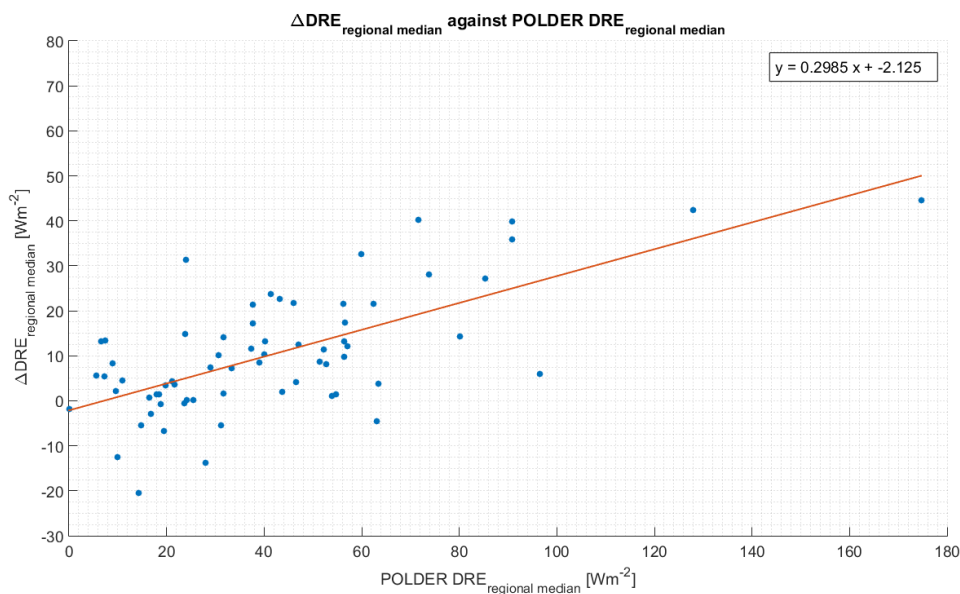


**Figure 14. A scatterplot of the difference in the ΔDRE_regional median, and the regional median DRE retrieved by POLDER. Each blue dot represents a day over which the regional median is calculated. The red line represents a linear relation that is fitted to the data using least squares. The fitted line suggests a positive linear relation between the ΔDRE_regional median and the DRE retrieved by POLDER.**

## 4.2 Aerosol optical thickness

Similar to the regional median DRE, a time series of the regional mean AOT is made, as is explained in section 3.6. The AOT is one of the main parameters that affect the DRE and it is expected that high AOT corresponds to high DRE for similar COT conditions.

A time series of the regional mean is made for an AOT at 550 nm and 1246 nm for overlapping data. This time series can be found in figure 15b and shows the regional mean AOT at 550 nm in red AOT at 1246 nm in blue. The DRE for overlapping data is shown in figure 15a as a reference. The mean $AOT_{regional\ mean}$ at 550 nm is 0.37 and the mean $AOT_{regional\ mean}$ at 1246 nm is 0.075. The highest values are reached on the 12th of August at 550 nm with a value of 1.1 and on the 15th of August at 1246 m with a value of 0.23. The three days used as case studies, the 11th of August, the 13th of August and the 19th of August, are marked in figure 15 with a vertical black line.
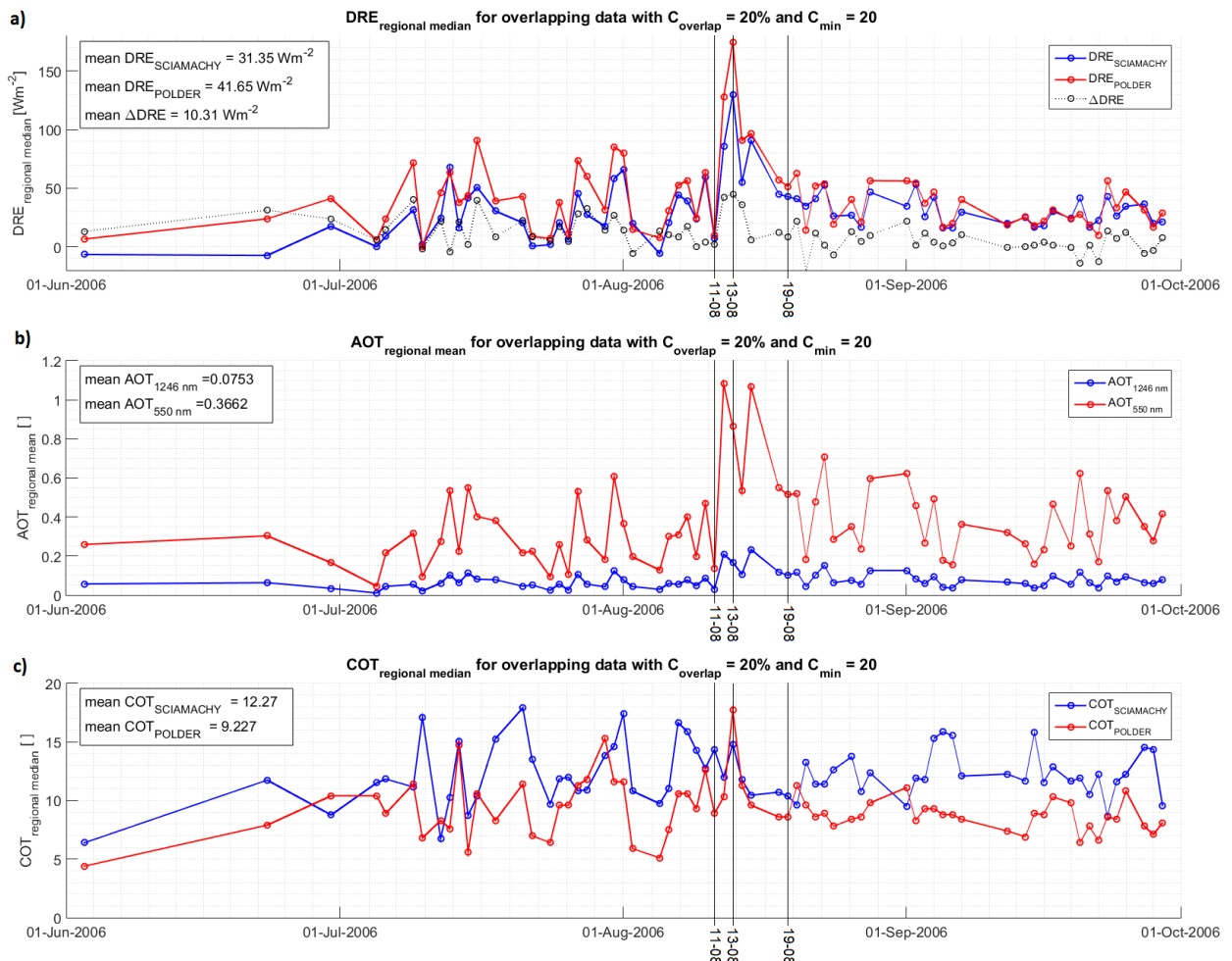


**Figure 15. (a) A time series of the regional median DRE by SCIAMACHY (blue) and POLDER (red) as well as the difference between the two, ΔDRE**$_{regional\ median}$**. (b) A time series of the POLDER retrieved regional mean AOT at 550 nm (red) as well as the AOT converted to 1246nm (blue). (c) A time series of the regional median COT retrieved by SCIAMACHY (blue) and POLDER (red). All three time series only consider overlapping data from the first of June until the 30**[th] **of September 2006 that satisfy conditions $C_{overlap}$ = 20% and $C_{min}$ = 20. Three days, the 11**[th] **of August, the 13**[th] **of August and the 19**[th] **of August 2006, are selected case studies and shown with the black vertical line.**

The regional mean AOT$_{550\,nm}$ generally shows the expected agreement with most DRE measurements; high AOT is found on days with high positive DRE. This can be seen in figure 15b and the relation is confirmed in figure 16. This figure contains two scatterplots of the regional median DRE of SCIAMACHY (figure 16a) and POLDER (figure 16b). The blue dots represent the retrieved regional median DRE and the red line is the linear relation that was fitted to the data using least squares. The fitted linear relation has a closer fit with the SCIAMACHY DRE, but for both instruments, the results are as expected: high AOT generally corresponds with high DRE. Deviations from this expectation are most likely a result of low COT values on those days.

While high AOT generally corresponds with high DRE, the maximum DRE on the 13th of August, is not found on the days with the highest AOT, which is on the 12th and 15th of August. The most likely cause of this is the other main parameter that affects the DRE: the COT, which is discussed in the next section.
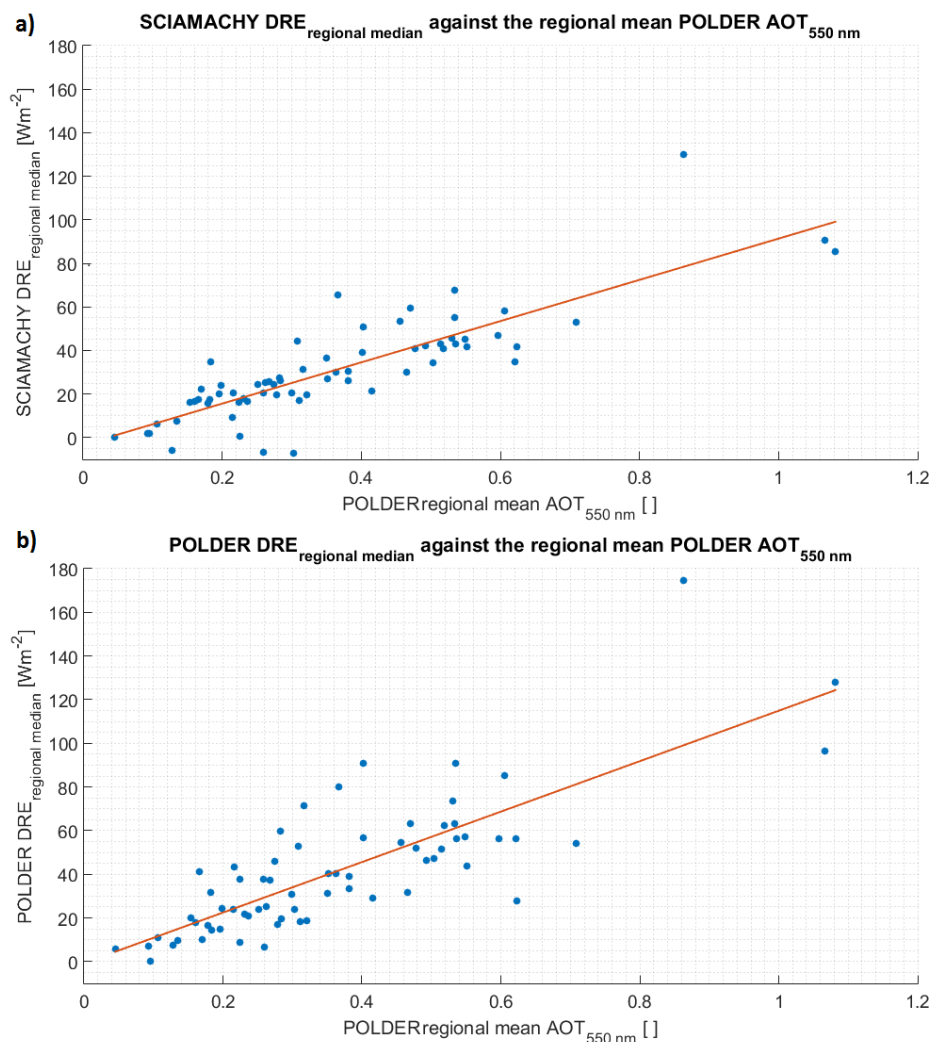


**Figure 16. (a) A scatterplot of the difference in SCIAMACHY regional median DRE, the regional mean AOT at 550 nm retrieved by POLDER. Each blue dot represents a day over which the regional median is calculated. The red line represents a linear relation that is fitted to the data using least squares. The fitted line suggests a positive linear relation between the SCIAMACHY regional median DRE and the AOT retrieved by POLDER. (b) A scatterplot of the difference in POLDER regional median DRE, the regional mean AOT at 550 nm retrieved by POLDER. Each blue dot represents a day over which the regional median is calculated. The red line represents a linear relation that is fitted to the data using least squares. The fitted line suggests a positive linear relation between the POLDER regional median DRE and the AOT retrieved by POLDER.**

## 4.3 Cloud optical thickness

Similar to the regional median DRE and the regional mean AOT, a time series of the regional median COT is made for retrieval by SCIAMACHY and POLDER. The COT is the other main parameter that affects the DRE and it is expected that high COT corresponds to high DRE for similar AOT conditions. In this study, the retrieved COT will be used mostly to understand the conditions in which the DRE is retrieved.

The time series of the overlapping COT, shown in figure 15c, shows the COT retrieved from SCIAMACHY in blue and the POLDER COT in red. In general, the SCIAMACHY COT is higher than the COT retrieved by POLDER, with overall means of 12.7 and 10.6 respectively. The maximum regional median COT are 17.9 for SCIAMACHY and 17.7 for POLDER, reached on the 21th of July and the 13th of August respectively.

The POLDER DRE and COT show agreement in figure 15c, i.e. high DRE is retrieved for days with high COT. This is especially visible on the 13th of August, where both the highest DRE and COT is retrieved with POLDER. However, the SCIAMACHY DRE and COT do not seem to show this agreement. There seems to be no relation between the SCIAMACHY DRE and COT, which is unexpected. The peak event in mid-August is a good example, where the retrieved DRE is very high, but the COT is only about average. Very high COT is retrieved in mid-July, while the retrieved DRE is quite low.

This result is further explored with scatterplots, shown in figure 17, of the regional median DRE against the regional median COT of both SCIAMACHY (figure 17a) and POLDER (figure 17b). These scatterplots show the regional median DRE as blue dots and the linear fit, made using least squares, as a red line. The linear fit in figure 17a is horizontal, showing that there is no relation between the SCIAMACHY COT and DRE. The linear fit of the POLDER retrieval in figure 17b does show the expected relation between the POLDER COT and DRE: a positive linear relation.

The relation between COT and DRE retrieval is hard to assess, because both the COT and the AOT need to be high in order to retrieve high DRE. High COT depends on the cloud development and is quite common in the region. High AOT is a result of a large biomass burning event on the African continent, in combination with an eastern wind, which less common. As a result, the relation between DRE and AOT is found more easily. It is possible to retrieve high COT, but low DRE. When the AOT is high, only moderate to high COT is needed to retrieve relatively high DRE. This can explain the results in both figure 15b and figure 17b. This however, only partially explains the poor relation between the SCIAMACHY DRE and COT. This will be further discussed in section 6.3, in which the COT is discusses as the third likely cause of the difference in DRE.
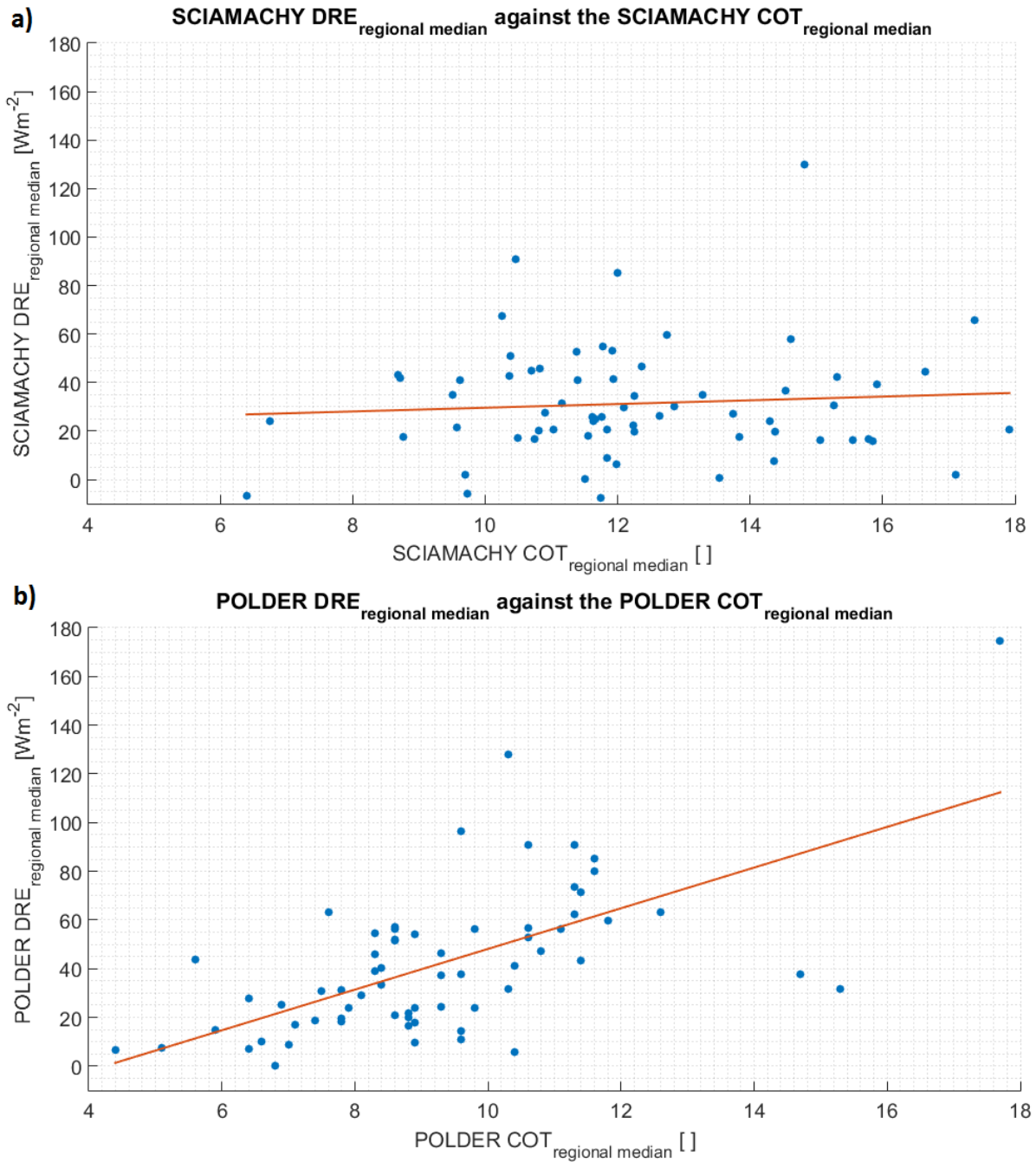
**Figure 17. (a) A scatterplot of the difference in SCIAMACHY regional median DRE, the regional median COT retrieved by SCIAMACHY. Each blue dot represents a day over which the regional median is calculated. The red line represents a linear relation that is fitted to the data using least squares. The linear fit is poor and suggests no relation between the SCIAMACHY regional median DRE and the COT retrieved by POLDER. (b) A scatterplot of the difference in POLDER regional median DRE, the regional mean COT retrieved by POLDER. Each blue dot represents a day over which the regional median is calculated. The red line represents a linear relation that is fitted to the data using least squares. The linear fit is weak but still suggests a positive linear relation between the POLDER regional median DRE and the COT retrieved by POLDER.**

# 5. Analysis

The time series that are shown in figure 15 are well suited for the comparison of the DRE retrieval of the two methods, but it does not give an understanding of the conditions during the retrieval. Understanding the processes involved is essential for understanding potential sources of the differences in the retrieved DRE. Three separate days will be discussed in this chapter. This will highlight the technical differences and/or explain some remarkable results in the time series.

Six images are shown in figures 19, 21 and 23 for each of the three case studies. These images show the DRE from SCIAMACHY (a) and POLDER (b), the COT from SCIAMACHY (c) and POLDER (d), the overlapping area of the two datasets (e) and the AOT from POLDER (f). The DRE, COT and AOT images also show the cloud conditions from MERIS and MODIS RGB imagery. The overlapping area of the two datasets in the figures (e) show the POLDER data in green, the overlapping POLDER data in red, the SCIAMACHY data in teal and the overlapping SCIAMACHY pixels have a black border. These figures are used to support the case studies, but only important or interesting features will be discussed. Note that the scales of the images might differ for each case.

For this chapter and the next, the month of August is an interesting month. There are a lot of days in August with overlapping data available and the three case studies are from August as well. That is why a new figure is made to support the data analysis in this chapter. This figure, figure 18, is similar to figure 15 in every way, but differs in that only the retrieval in August 2006 is shown. Figure 18a shows the time series of the regional median DRE from SCIAMACHY and POLDER, figure 18b shows the time series of the regional mean AOT form POLDER at 550nm and 1246 nm and finally figure 18c shows the COT from SCIAMACHY and POLDER.
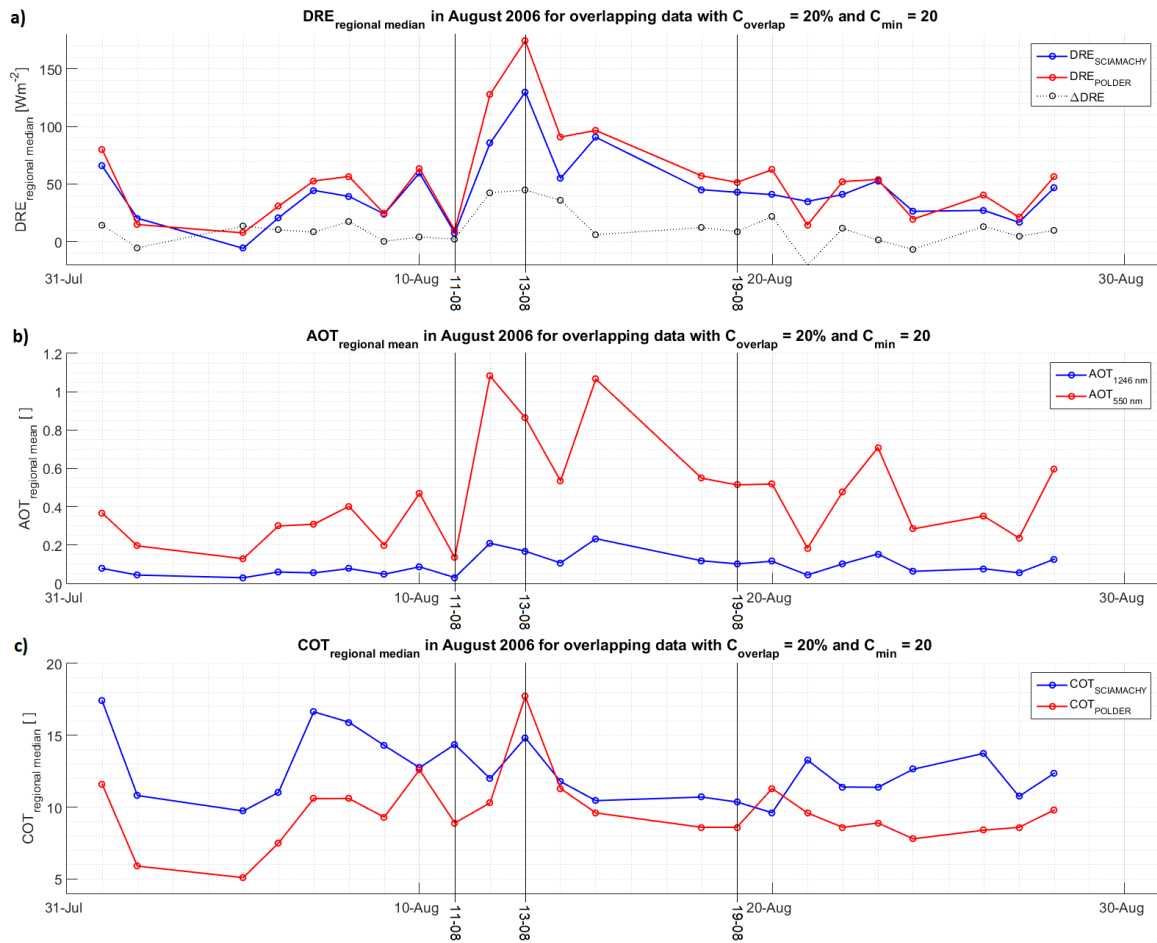
**Figure 18. (a)** A time series for August 2006 of the regional median DRE by SCIAMACHY (blue) and POLDER (red) as well as the difference between the two, $\Delta DRE_{regional\ median}$. **(b)** A time series for August 2006 of the POLDER retrieved regional mean AOT at 550 nm (red) as well as the AOT converted to 1246nm (blue). **(c)** A time series for August 2006 of the regional median COT retrieved by SCIAMACHY (blue) and POLDER (red). All three time series only consider overlapping data that satisfy conditions $C_{overlap} = 20\%$ and $C_{min} = 20$. Three days, the 11th of August, the 13th of August and the 19th of August 2006, are selected case studies and shown with the black vertical line.
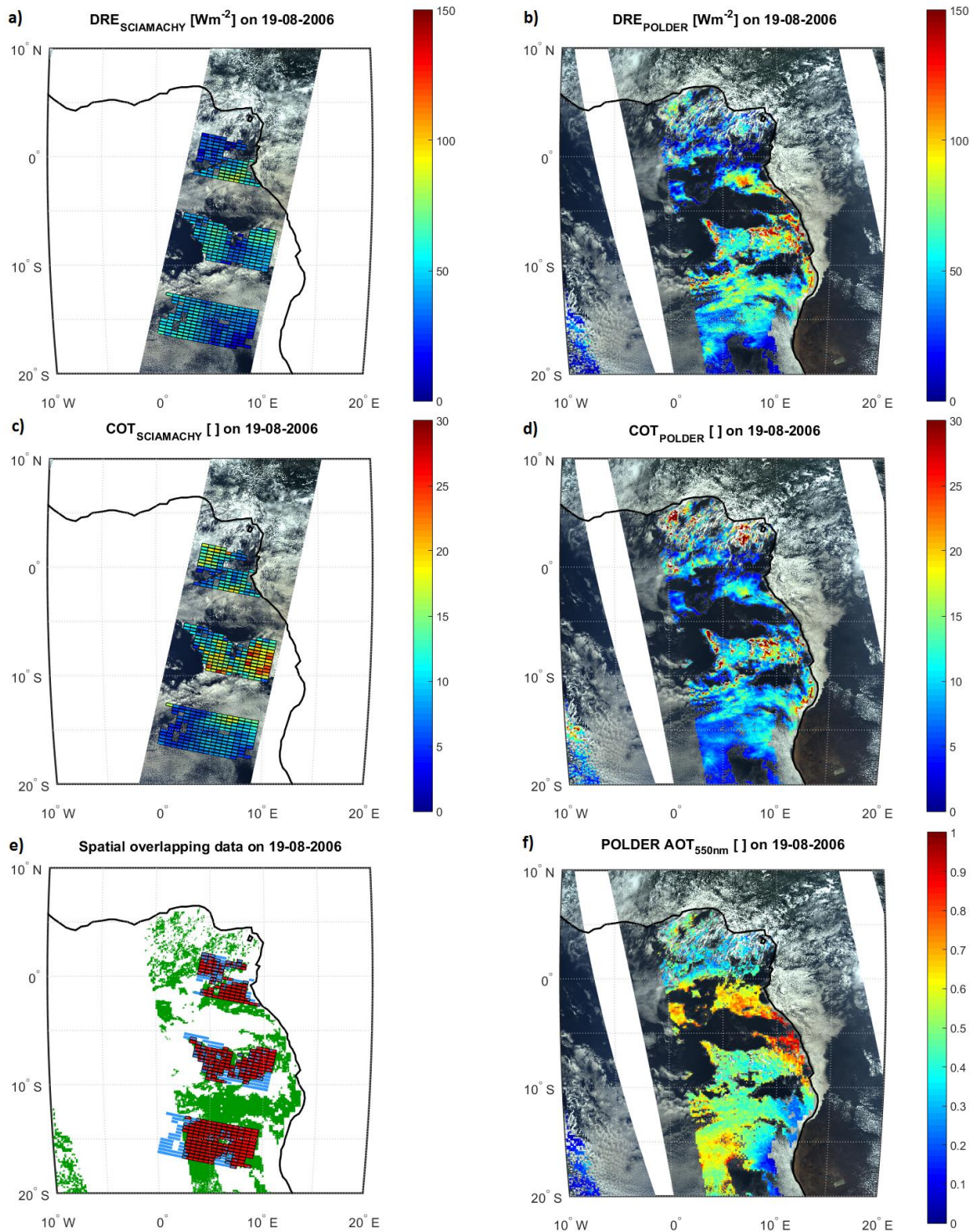
# 5.1 Case 1: 19 August 2006



**Figure 19.** (a) Cloud and smoke conditions on the 19th of August 2006, shown by MERIS RGB imagery, overlaid with SCIAMACHY DRE retrieval. (b) Cloud and smoke conditions on the 19th of August 2006, shown by MODIS RGB imagery, overlaid with POLDER DRE retrieval. (c) Cloud and smoke conditions on the 19th of August 2006, shown by MERIS RGB imagery, overlaid with SCIAMACHY COT retrieval. (d) Cloud and smoke conditions on the 19th of August 2006, shown by MODIS RGB imagery, overlaid with POLDER COT retrieval. (e) A visualization of all (green) and overlapping (red) POLDER retrieval and all (without border) and overlapping (black border) SCIAMACHY retrieval on the 19th of August 2006. (d) Cloud and smoke conditions on the 19th of August 2006, shown by MODIS RGB imagery, overlaid with POLDER AOT retrieval at 550 nm. The difference in overpass time between SCIAMACHY and POLDER is about 3.5 hours.

28

The 19th of August 2006 is especially suited to display the technical differences between the two methods because of the large area of overlap. As a reference: the regional median DRE for overlapping data is found in figure 18a at 45.1 Wm$^{-2}$ and 57.1 Wm$^{-2}$ for SCIAMACHY and POLDER respectively. The regional mean AOT on this day can be found in figure 18b at 0.51 and the regional median COT is 10.5 and 8.6 for SCIAMACHY and POLDER in figure 18c.

The retrieval of DRE can be found in figure 19a for SCIAMACHY and figure 19b for POLDER. The technical differences are clearly visible in this figure. Their effect is minimized by calculating the regional median DRE for overlapping pixels satisfying the conditions $C_{overlap}$ and $C_{min}$. The overlapping area is found in figure 19e, where overlapping POLDER data is red and overlapping SCIAMACHY data has a black border around each overlapping pixel.

An interesting feature that can be found on this day is the change in cloud cover as a result of the difference in overpass time. This major technical difference was already shown in figure 7, but it also has a strong effect on the 19th of August. The cloud cover is reduced between retrieval by SCIAMACHY and POLDER, as is highlighted in figure 20 which shows the COT retrieved by both instruments. Even though the COT retrieval seems similar, it is clearly visible in this figure that a large part of the cloud cover has dissolved when POLDER passes over the area. This highlights how much the cloud cover can change within a time span of 3.5 hours.
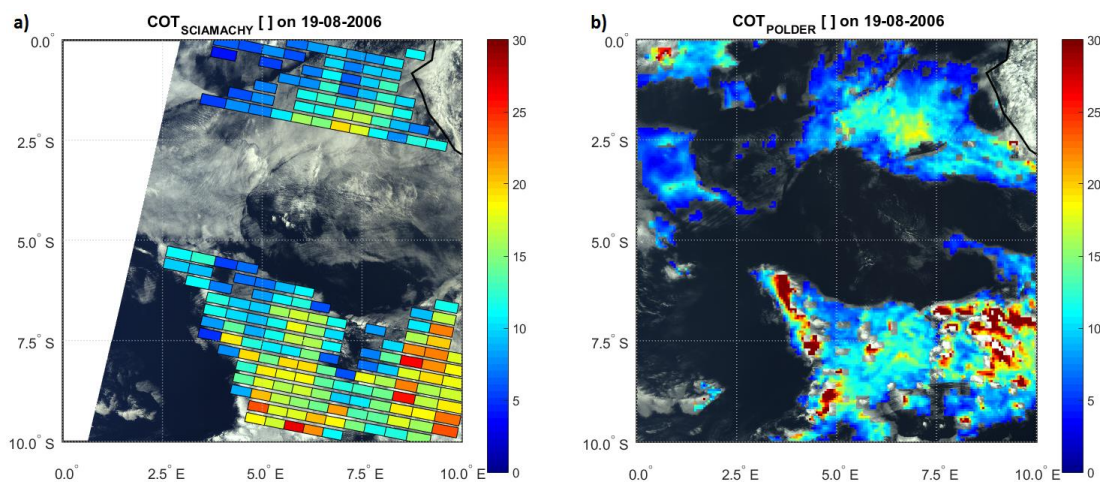


Figure 20. (a) The cloud and smoke conditions on the 19th of August 2006, shown by MERIS RGB imagery, overlaid with SCIAMACHY COT retrieval, for the region constraint between 0° and -10° latitude and 0° and 10° longitude. (b) The cloud and smoke conditions on the 19th of August 2006, shown by MODIS RGB imagery, overlaid with POLDER COT retrieval, for the region constraint between 0° and -10° latitude and 0° and 10° longitude.

Not only a large part of the cloud cover is dissolved, as shown in figure 20, but the regional median COT is also lower for POLDER than for SCIAMACHY. This change in cloud cover is a likely suspect for the changes in DRE retrieval, because a higher COT is associated with higher DRE. However, this is not what is found on this day. Both the regional median DRE for POLDER and SCIAMACHY, 45.1 Wm$^{-2}$ and 57.1 Wm$^{-2}$ respectively, and the DRE that is shown in figure 19a and 19b are higher for POLDER than for SCIAMACHY. The effect of the COT will be discussed further in section 6.3.
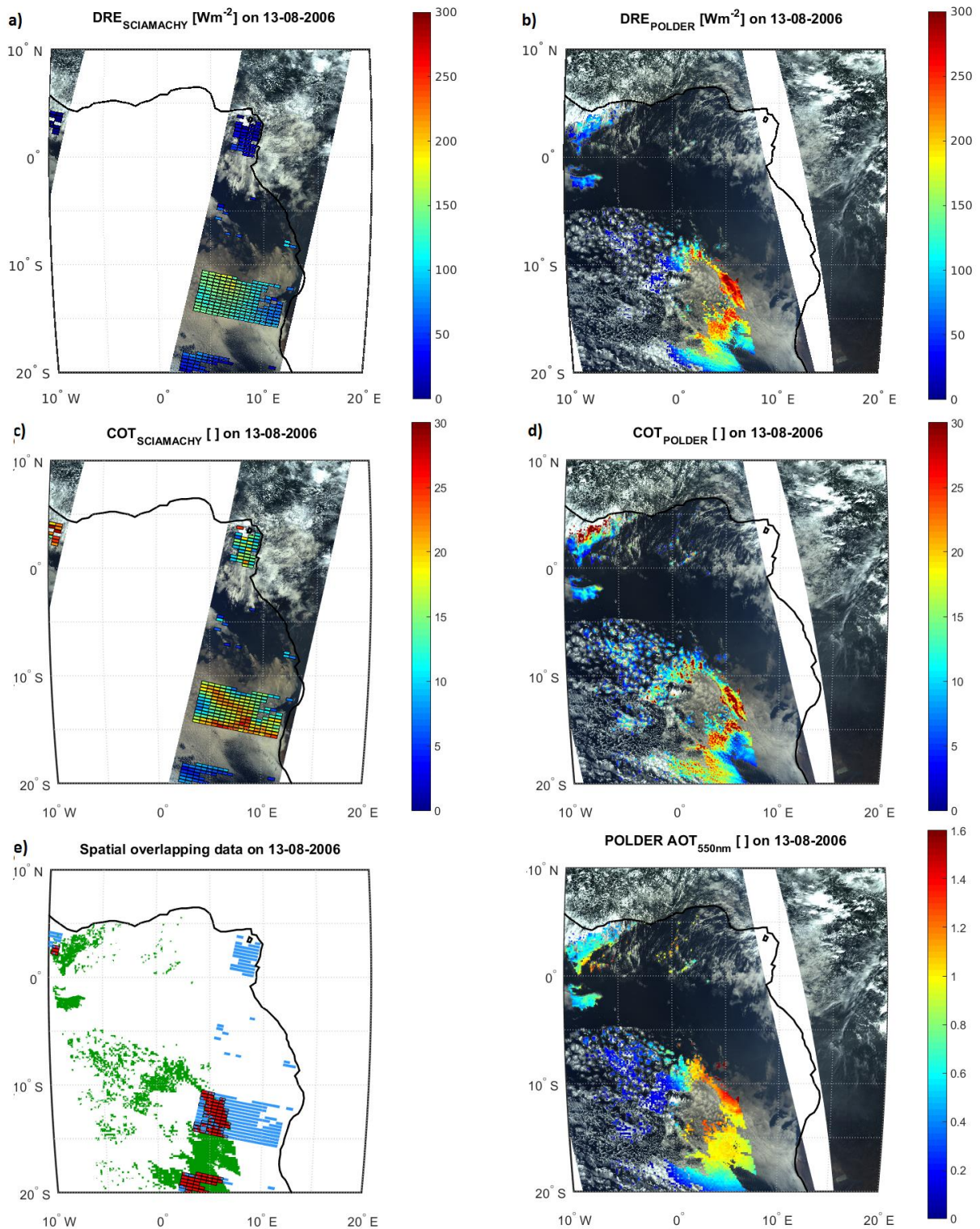
## 5.2 Case 2: the 13th of August



Figure 21. (a) Cloud and smoke conditions on the 13th of August 2006, shown by MERIS RGB imagery, overlaid with SCIAMACHY DRE retrieval. (b) Cloud and smoke conditions on the 13th of August 2006, shown by MODIS RGB imagery, overlaid with POLDER DRE retrieval. (c) Cloud and smoke conditions on the 13th of August 2006, shown by MERIS RGB imagery, overlaid with SCIAMACHY COT retrieval. (d) Cloud and smoke conditions on the 13th of August 2006, shown by MODIS RGB imagery, overlaid with POLDER COT retrieval. (e) A visualization of all (green) and overlapping (red) POLDER retrieval and all (without border) and overlapping (black border) SCIAMACHY retrieval on the 13th of August 2006. (d) Cloud and smoke conditions on the 13th of August 2006, shown by MODIS RGB imagery, overlaid with POLDER AOT retrieval at 550 nm. The difference in overpass time between SCIAMACHY and POLDER is about 3.5 hours.

The 13<sup>th</sup> of August 2006 has been described by many others when studying the DRE of above cloud aerosols, because of the high amount of absorbing aerosols that can be found on this day. This is a result of a large biomass burning event near the African coast in combination with easterly winds. During this comparison study, both methods retrieved the highest DRE on this day. The regional median DRE on this day, which can be found in figure 18a, is 130.0 $Wm^{-2}$ and 174.7 $Wm^{-2}$ for SCIAMACHY and POLDER respectively. The regional median COT for this day is found in figure 18c at 14.8 and 17.7 for SCIAMACHY and POLDER. The regional mean AOT for this day is found in figure 18b at 0.86.

The retrieved regional median DRE for overlapping data in figure 21a is very high as a result of multiple factors coming together. First, there are a lot of absorbing aerosols in the region as a result of the large biomass burning event, which results in very high AOT, shown in figure 21f. Secondly the COT is very high for both instruments as well, as can be seen in figure 21c and 21d. The regional median AOT is not highest on this day, as shown in figures 15b and 18b, but this combination of high COT and relatively AOT result in the exceptionally high DRE. The third and final reason is the overlap in the area. This is the same area where the highest AOT and COT is retrieved, as can be seen in figure 21e. The latter is clearly visible in figure 22, where the COT of both instruments (figure 22a and 22b), the overlapping area (figure 22c) and the AOT of POLDER (figure 22d) are shown for a smaller area. The combination of these three factors results in the very high regional median DRE for SCIAMACHY and POLDER.
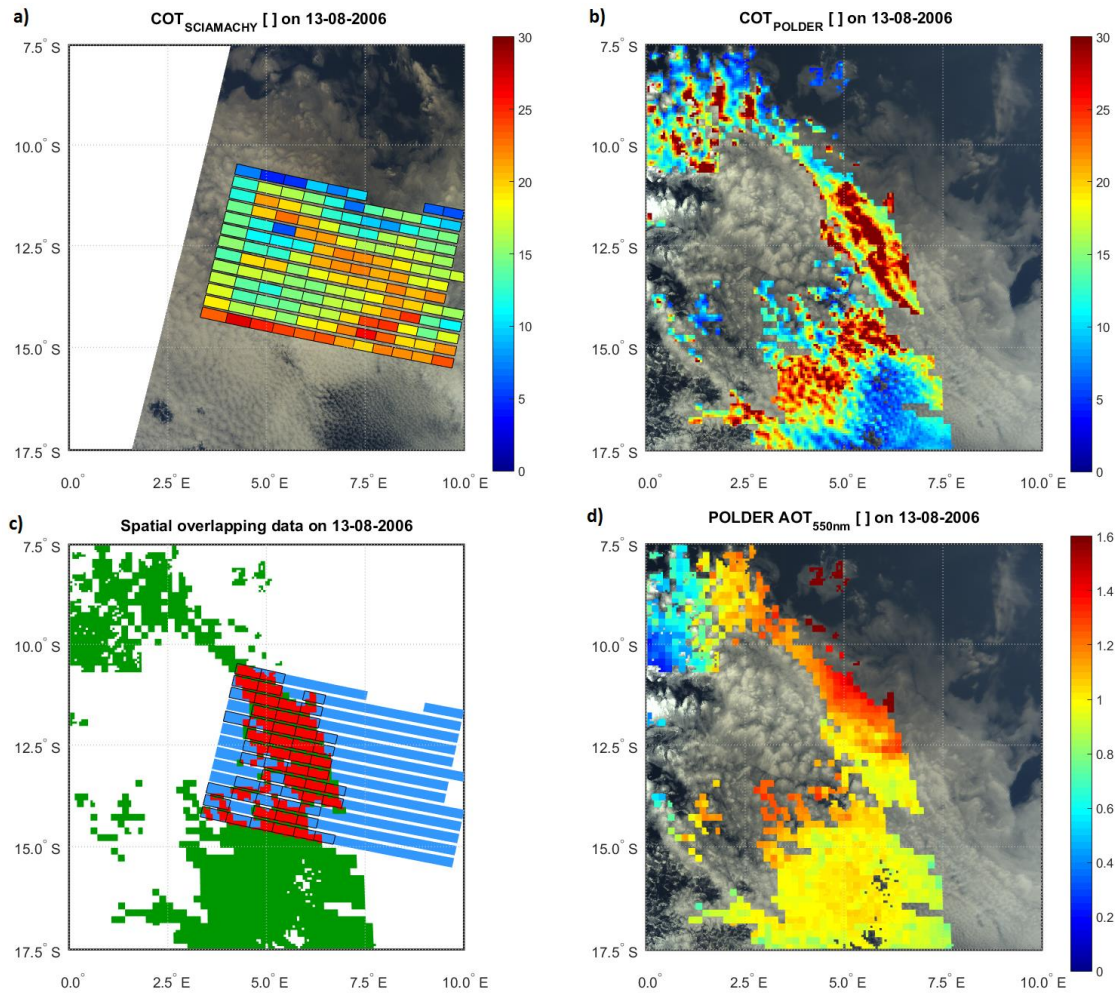
**Figure 22. (a) The cloud and smoke conditions on the 13th of August 2006, shown by MERIS RGB imagery, overlaid with SCIAMACHY COT retrieval, for the region constraint between -7.5° and -17.5° latitude and 0° and 10° longitude. (b) The cloud and smoke conditions on the 13th of August 2006, shown by MODIS RGB imagery, overlaid with POLDER COT retrieval, for the region constraint between -7.5° and -17.5° latitude and 0° and 10° longitude. (c) A visualization of all (green) and overlapping (red) POLDER retrieval and all (without border) and overlapping (black border) SCIAMACHY retrieval on the 13th of August 2006, for the region constraint between -7.5° and -17.5° latitude and 0° and 10° longitude. It can be seen that high COT for both instruments, as well as high AOT, is retrieved in the overlapping area. (d) Cloud and smoke conditions on the 13th of August 2006, shown by MODIS RGB imagery, overlaid with POLDER AOT retrieval at 550 nm, for the region constraint between -7.5° and -17.5° latitude and 0° and 10° longitude. The difference in overpass time between SCIAMACHY and POLDER is about 3.5 hours.**
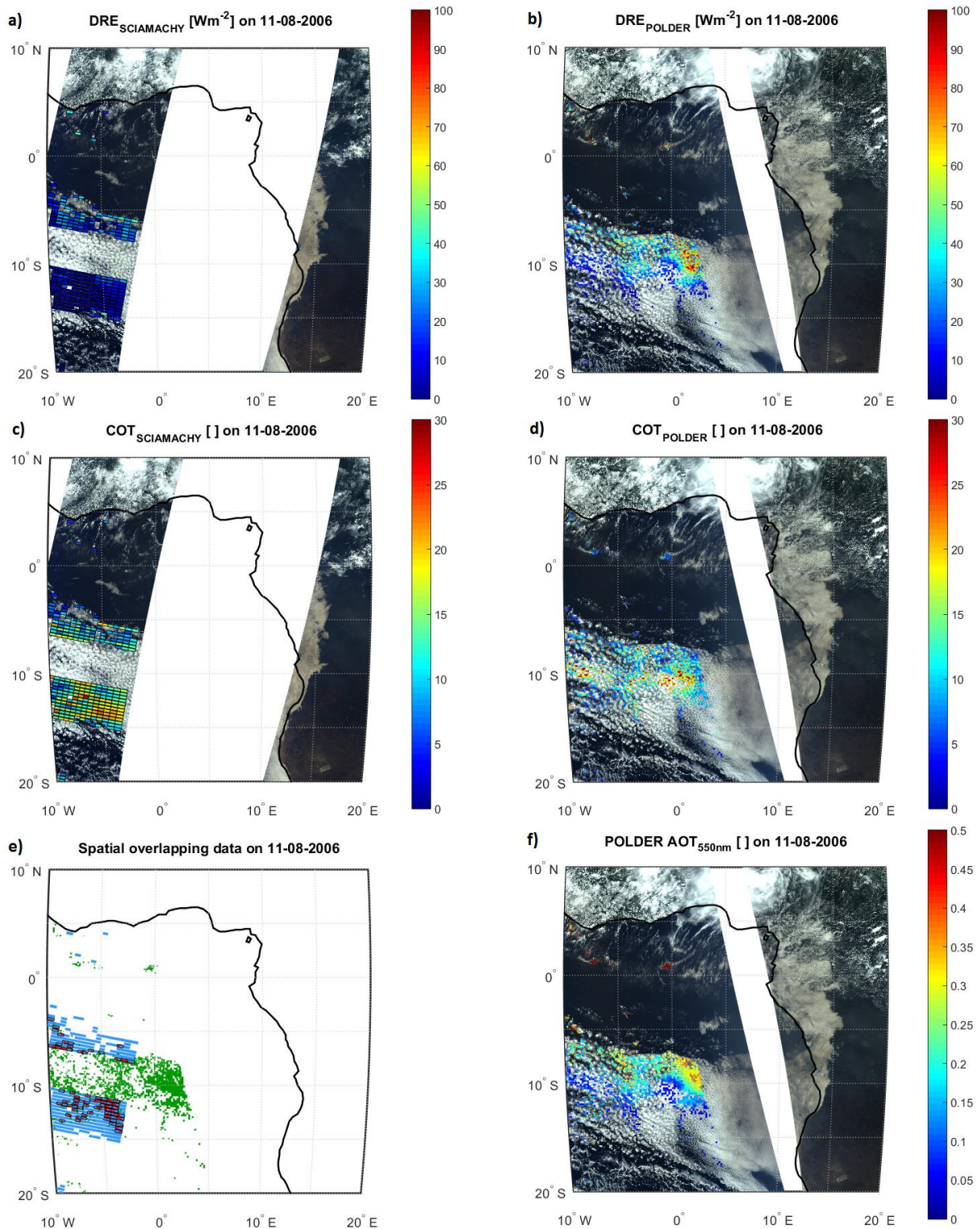
## 5.3 Case 3: the 11th of August



**Figure 23. (a)** Cloud and smoke conditions on the 11th of August 2006, shown by MERIS RGB imagery, overlaid with SCIAMACHY DRE retrieval. **(b)** Cloud and smoke conditions on the 11th of August 2006, shown by MODIS RGB imagery, overlaid with POLDER DRE retrieval. **(c)** Cloud and smoke conditions on the 11th of August 2006, shown by MERIS RGB imagery, overlaid with SCIAMACHY COT retrieval. **(d)** Cloud and smoke conditions on the 11th of August 2006, shown by MODIS RGB imagery, overlaid with POLDER COT retrieval. **(e)** A visualization of all (green) and overlapping (red) POLDER retrieval and all (without border) and overlapping (black border) SCIAMACHY retrieval on the 11th of August 2006. **(d)** Cloud and smoke conditions on the 11th of August 2006, shown by MODIS RGB imagery, overlaid with POLDER AOT retrieval at 550 nm. The difference in overpass time between SCIAMACHY and POLDER is about 3.5 hours.

33

When looking at the regional median DRE time series of figure 18a, the 11th of August stands out because of very low DRE for both instruments. This is especially unexpected, because very high regional median DRE is retrieved on the 12th and 13th of August. The regional median DRE on this day is only 7.4 $Wm^{-2}$ and 9.6 $Wm^{-2}$ for SCIAMACHY and POLDER respectively. The regional median COT, shown in figure 18c is 14.4 and 8.9 for SCIAMACHY and POLDER, which is about average. However, the regional mean AOT, shown in figure 18b, on the 11th of August is very low at only 0.13.

The conditions on the 11th of August are shown in figure 23. It can be seen that both instruments retrieve data in a region far from the coastline. The aerosols originate from biomass burnings on the mainland of Africa and it is expected that there is a reduction in AOT with distance from the west coast as a result of the relatively short lifetime of the aerosols. More importantly, the large plume of aerosols that is retrieved on the 12th and 13th of August has probably not traveled this far from the coast. As a result, the AOT is highest in the east. There are a couple of spots with high AOT in the north, but these are not taken into account because there is no overlap in that area.

The overlapping area between the two datasets is very small as well, especially compared to the 19th of August. The most likely cause for this is the broken cloud cover in the western region. The most important reason for the regional median DRE to be low for both instruments is that the overlap is located in a region with very low AOT. This is highlighted in figure 24, where figure 24a shows the overlapping area and figure 24b the AOT from POLDER.
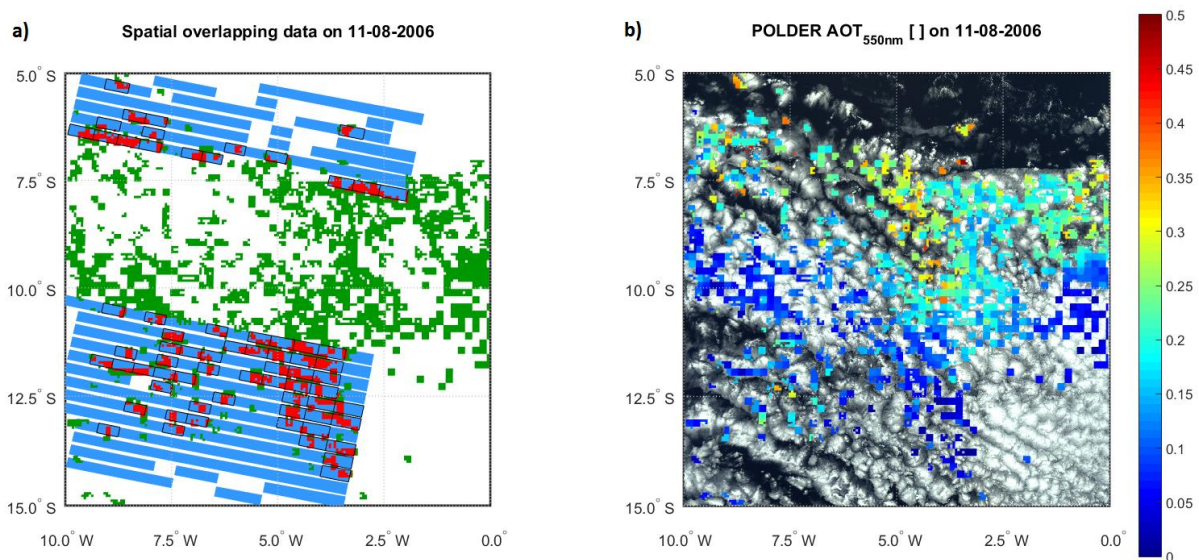


**Figure 24. (a) A visualization of all (green) and overlapping (red) POLDER retrieval and all (without border) and overlapping (black border) SCIAMACHY retrieval on the 11th of August 2006, for the region between -5° and -15° latitude and -10° and 0° longitude. (b) Cloud and smoke conditions on the 11th of August 2006, shown by MODIS RGB imagery, overlaid with POLDER AOT retrieval at 550 nm, for the region between -5° and -15° latitude and -10° and 0° longitude. This figure shows that there is a small amount of overlap on this day and that most overlap is in a region with very low AOT.**

This example shows that the regional median DRE that is shown in figure 18a is very much dependent on sampling of the instruments. When the overlapping area corresponds with an area of high AOT and high COT, as is the case on the 13th of August, high regional median DRE will be retrieved by both instruments. It also works the other way. When the overlapping area corresponds with an area of low AOT, like on the 11th of August, the regional median DRE is low for both instruments.

# 6. Discussion

This chapter will discuss three potential sources of the remaining difference that is shown in figures 13b, 15a and 18a. Three likely causes are defined as statements and tested if they are true or false. The assumption of the SCIAMACHY method that the AOT at 1246 nm is negligible is the first likely cause of the difference in DRE. An overestimation of the AOT retrieval by POLDER is the second likely cause of the difference in DRE that will be discussed. Finally, high POLDER COT retrieval compared to SCIAMACHY is suspected to be a large cause of the discrepancy between DRE from both instruments.

## 6.1 Cause 1: SCIAMACHY underestimates the DRE by neglecting the AOT at 1246 nm.

The SCIAMACHY method models the unpolluted cloud spectrum by retrieving cloud properties at 1246 nm and 1640 nm. It is assumed that the $AOT_{1246\,nm}$ is zero. If the signal at this wavelength is contaminated with aerosols, the cloud properties retrieved by SCIAMACHY will be biased, resulting in an impact on the modeled unpolluted TOA reflectance. This can cause an underestimation of the retrieved DRE.

SCIAMACHY does not retrieve the AOT at any wavelength. For this analysis, the $AOT_{550\,nm}$ retrieved by POLDER is used and converted to the $AOT_{1246\,nm}$, as described in the "Methodology". It is assumed that the effect of the difference in overpass time between the instruments is negligible.

The effect of the residual $AOT_{1246\,nm}$ was quantified by *De Graaf et al.* (2012). In a case study on the 10th of August 2006, it was found that an $AOT_{1246\,nm}$ of 0.046 caused an underestimation of the retrieved DRE by about 1 Wm$^{-2}$. This underestimation is proportional to the $AOT_{1246\,nm}$ [*De Graaf et al.*, 2012]. The results of this case study will be applied to the converted $AOT_{1246\,nm}$ to give a rough approximation of the underestimation effect of the $AOT_{1246\,nm}$ on the DRE, the $DRE_{underestimation}$.
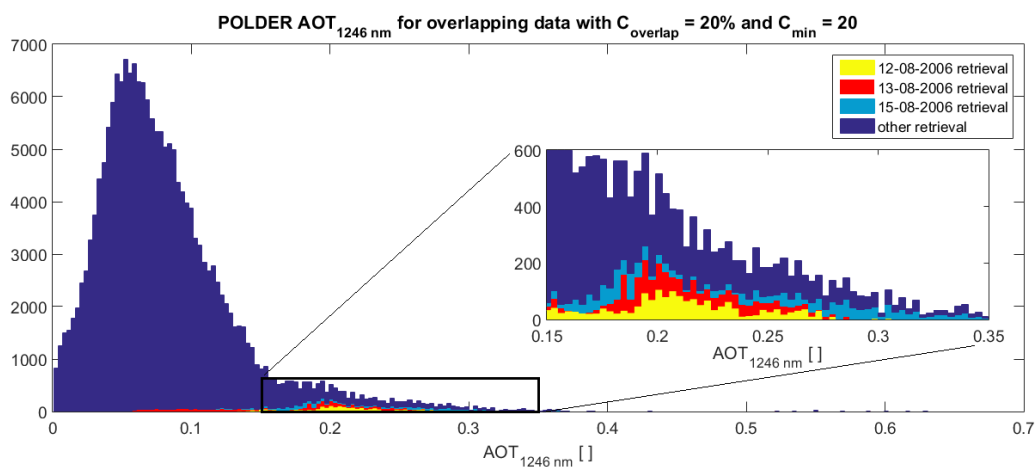


**Figure 25. A histogram of all overlapping AOT data, converted from 550 nm to 1246 nm. The overlap is determined with C$_{overlap}$ of 20% and C$_{min}$ of 20. Most of the retrieved AOT is found between 0 and 0.15, with a peak close to 0.05. A long tail of high AOT retrieval can be seen between 0.15 and 0.35, with some values reaching values up to 0.63. The total heights of the bars show the total amount of retrievals at each wavelength. The colors indicate which part of the data is retrieved on a certain day. The 12th of August is yellow, the 13th of August is red and the 15th of August is light blue. All other days are dark blue. The figure also shows a detailed image of the retrieval between 0.15 and 0.35. This shows that most of the AOT$_{1246}$ is retrieved on just a few days with high loadings of absorbing aerosols**

The histogram of figure 25 shows the converted $AOT_{1246\ nm}$ for all overlapping pixels that was used to calculate this regional mean $AOT_{1246\ nm}$ of figure 15b. The total mean $AOT_{1246\ nm}$ of 0.078 results in an approximate average DRE underestimation of 1.7 $Wm^{-2}$. About 2.3 % of all $AOT_{1246\ nm}$ data are higher than 0.2 which results in an underestimation larger than 4 $Wm^{-2}$.

The underestimation is strongest on days with high loadings of absorbing aerosols. Most of the high $AOT_{1246\ nm}$ retrievals from figure 25 are retrieved in just a few days where the aerosol load was high. To show this in figure 25, the three days with the highest regional mean $AOT_{1246\ nm}$ are shown in yellow, red and light blue. This shows that more than half of all DRE above 0.2 is retrieved on just these three days. As a result, the underestimation will be strongest on just e few days with high AOT retrieval.

To give an approximation of the underestimation, a regional median underestimation time series is calculated, based on the previously mentioned case study by *De Graaf et al.* (2012) and the regional mean $AOT_{1246\ nm}$. This time series is shown in figure 26, where the time series over the full time period is shown in figure 26a and only August 2006 is shown in figure 26b. On average over the full time period, the $DRE_{underestimation}$ is only 1.57 $Wm^{-2}$, which is 5% of SCIAMACHY DRE of 31.5 $Wm^{-2}$. This is small and the underestimation is hardly visible in both figure 26a and 26b. However, 1.56 $Wm^{-2}$ is about 15% of the mean of the DRE difference between SCIAMACHY and POLDER of 10.31 $Wm^{-2}$ over the whole time period. This shows that a small underestimation can explain a significant portion of the difference in DRE.
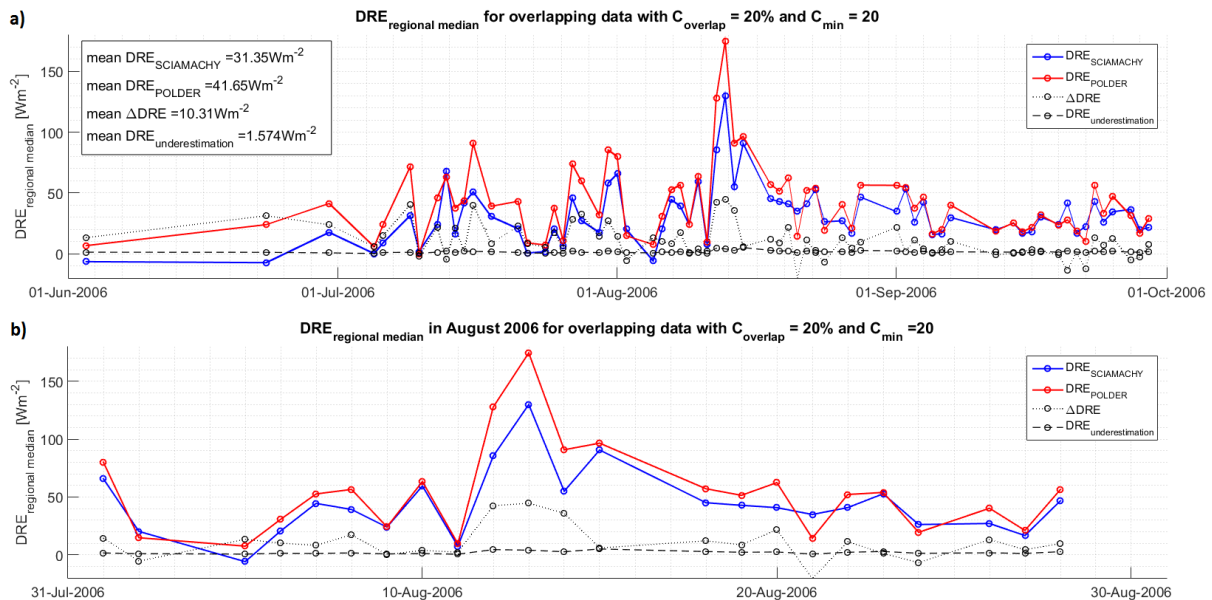


Figure 26. (a) A time series for the first of June to the 30th of September 2006 of the regional median DRE by SCIAMACHY (blue) and POLDER (red), the difference between the two, $\Delta DRE_{regional\ median}$ (dotted black) and the estimated underestimation by SCIAMACHY (dashed black). (b) A time series for August 2006 of the regional median DRE by SCIAMACHY (blue) and POLDER (red), the difference between the two, $\Delta DRE_{regional\ median}$ (dotted black) and the estimated underestimation by SCIAMACHY (dashed black). This figure shows that the underestimation is very small with a mean of 1.57 $Wm^{-2}$, but this is about 15% of the mean $\Delta DRE_{regional\ median}$ of 10.31 $Wm^{-2}$.

The approximations of the $DRE_{underestimation}$ are based on multiple assumptions and uncertainties. The first assumption is that the effect of the overpass time difference on the AOT is negligible. The second assumption states that the Ångström exponent used in equation 5 is independent of wavelength and aerosol type, which may change over the course of a few days. Finally, it is assumed

that the relation between the $AOT_{1246\,nm}$ and $DRE_{underestimation}$ is only dependent on the AOT, since it is based on a single day of SCIAMACHY retrieval.

It can be concluded that residual AOT at 1246 nm cannot be neglected and that this is indeed a partial cause of the DRE difference. Over the whole time period, the underestimation of the DRE is expected to be about 5% of the SCIAMACHY DRE on average, but this is approximately 15% of the $\Delta DRE_{regional\ median}$. This is a rough approximation and it is recommended that further research is done on the subject.

## 6.2 Cause 2: POLDER retrieves higher positive DRE as a result of an overestimation of the AOT.

The DRE retrieved by POLDER is strongly dependent on the retrieved AOT, where high AOT naturally corresponds with high positive DRE over clouds. In order to see if POLDER overestimates the AOT, the retrieved AOT by *Peers et al.* (2015) is compared with the results of the inter-comparison of retrieval of above cloud aerosol optical thickness (ACAOT) by A-train sensors, by *Jethva et al.* (2013), which is one of the very few comparison studies in this field.

The comparison study by *Jethva et al.* (2013) uses retrieval on two days, including the 13th of August 2006. The retrieved AOT by each sensor is shown in a spatial plot as well as a comparative plot along the CALIOP track, which are all shown in figure 1 of *Jethva et al*. (2013). In this section, conclusions are drawn from this figure on the difference between POLDER DRE retrieval compared to MODIS and OMI DRE retrieval. The spatial plot of POLDER AOT for the 13th of August 2006, shown in the top right of figure 1 by *Jethva et al.* (2013), will be replicated in figure 27 for comparison.

The comparison by *Jethva et al.* (2013) shows, in the comparative plot at the bottom of their first figure, that POLDER generally retrieves higher AOT than other sensors. In contrary to what is said in the article, large differences (up to 0.5) can be observed between the POLDER AOT and the AOT retrieved by OMI and MODIS for AOT values higher than 1. This is can be found between -15° and -10° latitude in the comparative plot of their first figure [*Jethva et al.,* 2013].

The differences between the AOT retrieved by POLDER and the other instruments can be a result of many factors. Each method relies on different assumptions which can affect the accuracy. For example, both the MODIS and OMI algorithms consider one model of aerosols (i.e. size distribution, refractive index) [*Jethva et al.*, 2013], while the POLDER algorithm considers multiple models [*Peers et al.*, 2015]. The POLDER algorithm assumes that the polarized measurements are not affected by aerosol absorption, in order to retrieve the AOT. This is an assumption, which becomes less consistent when the aerosol layer is very absorbing, is a potential source of bias for large absorbing aerosol loads [*Peers et al.,* 2015].

The comparison of *Jethva et al.* (2013) was done for the AOT at 500 nm. To compare the AOT retrieved in the study of *Peers et al* (2015), it is converted to 500 nm using equation 5. Figure 27 shows the $AOT_{500\,nm}$ for the 13th of August 2006. The scale limits in figure 27 are set to zero and 1.6, the same limits used in figure 1 of *Jethva et al.* (2013) in order to compare the two images.

The AOT of figure 27 shows very good agreement with the POLDER retrieval in the first figure by *Jethva et al.* (2013). There are small differences between the two, because the POLDER

measurements have been recalibrated and because of an improvement of the POLDER algorithm in order to retrieve the DRE. This new version does include absorption by aerosols [*Peers et al.* (2015)]. The most noticeable difference is the large gap in the data, which is highlighted by the red square in figure 27a, which could be a result of a change in the filter on the cloud heterogeneity. As a result of the changes, the figure 27 seems to show an increase in $AOT_{500\,nm}$ compared to the first figure of *Jethva et al.* (2013). This is an increase on top of the already relatively high POLDER AOT by *Jethva et al.* (2013).
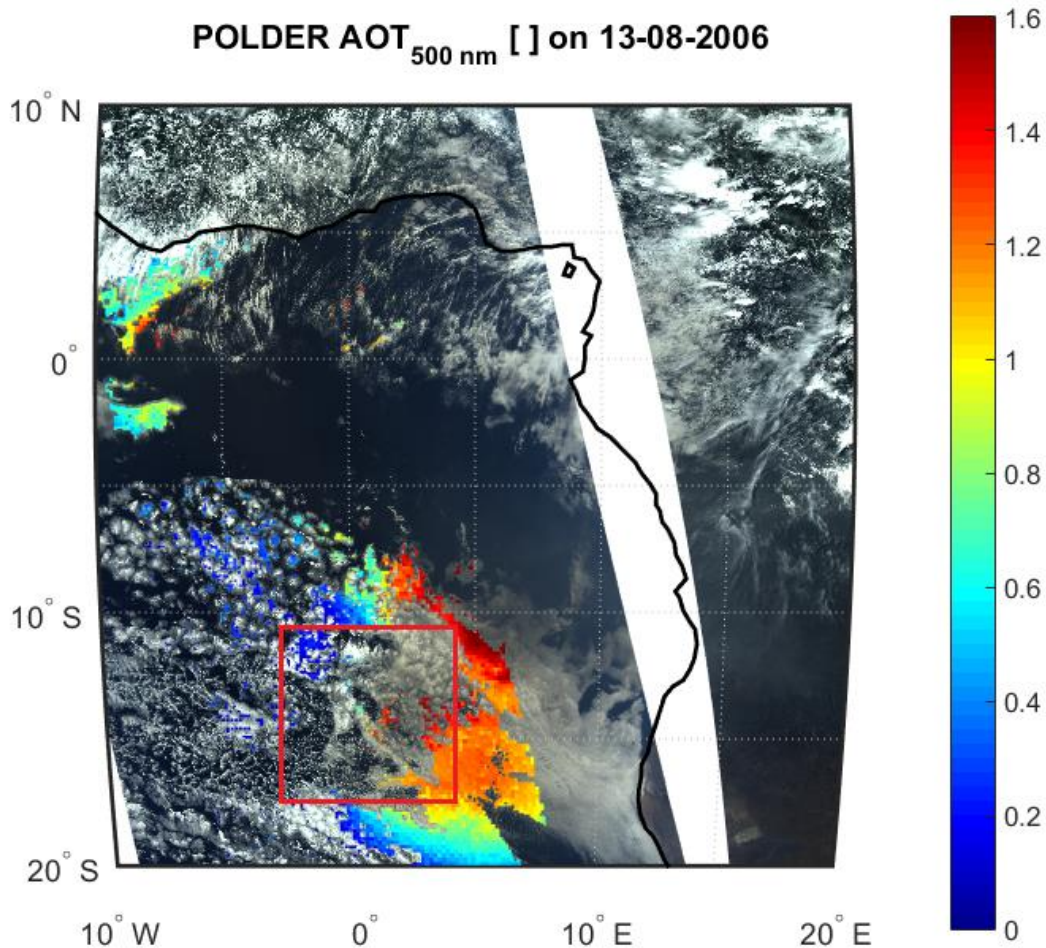


**Figure 27. The cloud and smoke conditions on the 13th of August 2006, shown by MODIS RGB imagery, overlaid with POLDER $AOT_{550nm}$ retrieval. POLDER and MODIS pass over the area in the South East Atlantic in ascending orbit in the early afternoon. The red rectangle highlights a large gap in the data. This gap is not visible in figure 1 of *Jethva et al.* (2013) and could be a result of a change in the filter on the cloud heterogeneity.**

Assessing the accuracy of the aerosol properties above clouds derived by satellite is challenging. The results from both *Jethva et al.* (2013) and this study show that POLDER is on the high side when retrieving both AOT and DRE of above cloud aerosols. POLDER calculates the DRE by accurately retrieving aerosol properties for moderate aerosol concentrations, with only few assumptions. However, a potential bias is introduced when the aerosol layer is very absorbing. The sensitivity study by *Peers et al* (2015) is done until a maximum AOT of 0.6, a value that was exceeded many times in 2006. Therefore, it is still uncertain how strong the bias is, if there is any, for retrieval when the aerosol layer is very absorbing. It is recommended that more research is done on the accuracy of the AOT retrieval by POLDER. As a result, this is deemed to be a likely cause of the DRE difference, but the magnitude of the effect is uncertain.

## 6.3 Cause 3: POLDER retrieves higher positive DRE as a result of higher COT retrieval.

The COT has a very strong effect on the DRE, where increasing COT results in increasingly positive DRE for similar AOT conditions. The systematically larger DRE that is retrieved by POLDER can be explained by a systematically higher COT. The COT retrieved by both methods is compared, in order to find anything out of the ordinary that can explain the difference in DRE. The COT is retrieved by the two instruments with very different methods and a quantitative comparison could be a full study by itself. To study if the DRE difference is indeed caused by a higher POLDER COT, the COT is compared qualitatively to understand the processes that lead to the retrieved DRE.

The COT retrieval is shown in the histograms of figure 10 in section 3.5, which shows all COT retrieval in overlapping areas. These histograms show that the COT retrieved by SCIAMACHY is generally higher than the COT of POLDER, with median COT of 12.0 and 9.3 respectively. POLDER retrieves higher peak values than SCIAMACHY, due to its higher resolution.

The POLDER histogram shows that indeed only COT > 3.0 is included in the DRE retrieval and that all values larger than 42 are set to 42. This is a result of the limits of the LUT used to determine the COT. This does affect the mean and standard deviation of the histogram, but it has a negligible effect on the median of the COT retrieval. The spikes that are visible in the POLDER COT of figure 12b are a result of the discrete sampling of the LUT, done to retrieve the COT from POLDER measurements.

The same result of high SCIAMACHY COT retrieval and low POLDER COT retrieval is seen in the time series of the regional median COT for both instruments. The time series from June 2006 to October 2006 is shown in figure 15c and the time series for only August 2006 is shown in figure 18c. During the majority of days in both figures, the regional median COT of SCIAMACHY is significantly larger. This can be a result of the cloud cover being systematically thicker in the morning, when SCIAMACHY retrieves the COT [*Bergman et al.,* 1996]. That is indeed what is found in the case studies of the 11th of August and the 19th of August and is highlighted in figures 7 and 20.

Interestingly, the $\Delta DRE_{regional\ median}$ seems to be systematically smaller when the COT of SCIAMACHY is larger than the COT of POLDER. This is especially visible at the beginning of August, in figure 15 and 18, and in September in figure 15. Under the same aerosol conditions, higher COT is associated with higher DRE, but the retrieved DRE from POLDER is still slightly larger despite the lower COT. The fact that a higher COT retrieval by SCIAMACHY results in better agreement in DRE retrieval suggests that there might be a systematic DRE difference. The effect of higher SCIAMACHY COT possibly cancels out this systematic DRE difference, resulting in close agreement.

The SCIAMACHY retrieval does not show the expected relation, i.e. high DRE is retrieved on days with high COT. This is described in section 4.3, where no agreement was found in the time series of figure 15 and no relation was found in the scatterplot of figure 17a. The most likely explanation for this unexpected result is a combination of the low resolution of SCIAMACHY and the retrieval condition, i.e. only data is considered with CF > 0.3. This combination allows for retrieval of partly clouded areas, which might be compensated by the COT.

It is very difficult to compare the COT retrieval of the two instruments, because of the use of very different methods, the large difference in resolutions and the evolution of the cloud cover in the time between retrieval by the instruments. Both estimated COT results can be close to the truth and the

differences are sufficiently large for a qualitative analysis. From the results, it is concluded that a high POLDER COT is not the cause of the difference in DRE. The overall POLDER COT is lower than the SCIAMACHY COT and cannot explain the differences in DRE. From the results of this study, it seems that the effect of the difference in COT on the DRE is actually about equivalent to a possible systematic DRE difference. However, the comparison of the COT retrieval by SCIAMACHY and POLDER is worth its own study and it is recommended that further research is done on this topic as well.

# 7.  Conclusion

In this study the DRE of ACA, retrieved from satellite measurements by two unique methods, are compared from the first of June until the 30th of September 2006 over the South East Atlantic. Both methods aim to only retrieve positive DRE by only considering measurements over clouds. The first method models the unpolluted cloud spectra and compares this modeled reflectance with reflectance measurements from SCIAMACHY/Envisat. The strength of this method is that it avoids assumptions on aerosol properties. The second method uses multi-angle total and polarized radiances, measured with POLDER/PARASOL, to retrieve aerosol and cloud properties from which the DRE can be retrieved. The strength of this method is the independent retrieval of aerosol properties. For each day, the median DRE is calculated over the full region. This regional median DRE is used to make a time series, which is the main method of comparing the DRE of both methods.

A specific cause of difference in DRE retrieval is defined as the technical differences, which result in a discrepancy in DRE retrieval that can be minimized. Technical differences are the result of the limitations of the instrument or the limitations of the retrieval method. Two major problems for comparison are caused by technical differences: retrieval of DRE at different locations and at different times. The problem of different locations is minimized by only considering overlapping data. This is used to quantify the effect of the technical differences. The latter problem cannot be quantified, but is taken into account when analyzing the effect of the DRE differences that remain after the minimization of technical differences.

Data is considered to overlap when 20% of each large SCIAMACHY pixel is filled with smaller POLDER pixels. The effect of technical differences is minimized by calculating the regional median DRE per day for overlapping data, with a minimum of 20 overlapping SCIAMACHY pixels per day. High positive DRE is retrieved for overlapping data, with a mean regional median DRE of 31.4 Wm$^{-2}$ and 41.7 Wm$^{-2}$ for SCIAMACHY and POLDER respectively. As a result of the overlap, the mean DRE difference, or mean $\Delta DRE_{regional\ median}$, is reduced from 16.9 Wm$^{-2}$ to 10.3 Wm$^{-2}$. The technical differences are estimated to cause 6.6 Wm$^{-2}$, or 39% of the mean $\Delta DRE_{regional\ median}$ of all data.

The DRE time series for overlapping data of both methods show improved agreement for days associated with high positive DRE. The most likely suspects for the remaining $\Delta DRE_{regional\ median}$ for overlapping data are an underestimation by SCIAMACHY, an overestimation of the AOT by POLDER and discrepancy in the retrieved COT by both instruments.

It is concluded that the SCIAMACHY method underestimates the DRE by approximately 5% by assuming that the AOT is zero at 1246 nm. The mean underestimation of the regional median DRE by SCIAMACHY is estimated at 1.6 Wm$^{-2}$. Even though this is only 5% of the SCIAMACHY DRE, it causes approximately 15% of the remaining mean $\Delta DRE_{regional\ median}$ for overlapping data. The DRE and AOT retrieval by POLDER is concluded to be relatively high, compared to other instruments. An overestimation of the AOT, and therefore of the DRE, is expected, but more research is required to quantify the expected overestimation. In general, higher COT is retrieved by SCIAMACHY than by POLDER. However, SCIAMACHY still retrieves lower DRE. The DRE of both instruments agrees best when the COT of SCIAMACHY is larger than the POLDER COT, suggesting a systematic bias in the DRE.

The SCIAMACHY method is recommended to correct for the residual AOT at 1246 nm, by retrieving cloud properties at higher wavelengths or by estimating the AOT contamination with AOT retrieval from other instruments. It is recommended to apply the SCIAMACHY method to an instrument with a higher spatial resolution, which is likely to be the biggest downside of the method. POLDER retrieves high AOT and DRE when compared to other instruments. It is recommended that more research is done on the accuracy of the retrieval of aerosol properties for event where the aerosol layer is very absorbing.

This level of absorption by aerosols is expected to have a large effect on cloud development and the vertical stability of the atmosphere. The impact of the DRE has to be quantified in further studies. This study does confirm that these two methods are viable for retrieving the DRE of ACA.

# References

[1]    Bergman, J.W. and Salby, M.L.: Diurnal variations of cloud cover and their relationship to climatological conditions. *Journal of climate*, *9*(11), pp.2802-2820, 1996

[2]    Bovensmann, H., Burrows, J. P.,Buchwitz, M., Frerick, J., Noël, S., Rozanov, V. V., Chance, K. V., Goede, A. P. H.: SCIAMACHY: Mission objectives and measurement modes, Journal  of the Atmospheric  Sciences, 56(2), 127–150, doi:10.1175/1520-0469, 1999.

[3]    De Graaf, M., Tilstra, L. G., Wang, P., and Stammes, P.: Retrieval of the aerosol direct radiative effect over clouds from spaceborne spectrometry, Journal of Geophysical Research-Atmos., 117, D07207, doi:10.1029/2011JD017160, 2012.

[4]    Deschamps, P. Y., Breon, F. M., Leroy, M., Podaire, A., Bricaud, A., Buriez, J. C., Seze, G.: The POLDER mission: instrument characteristics and scientific objectives, IEEE Transactions on Geoscience and Remote Sensing, 32(3), 598-615, doi:10.1109/36.297978, 1994.

[5]    Forster, P., et al. (2007), Changes in atmospheric constituents and in radiative forcing, in Climate Change 2007: The Physical Science Basis. Contribution of Working Group I to the Fourth Assessment Report of the Intergovernmental Panel on Climate Change, edited by S. Solomon et al., pp. 129–234, Cambridge Univ. Press, Cambridge, U. K.

[6]    Jethva, H., Torres, O., Waquet, F., Chand, D., Hu, Y.: How do A-train sensors intercompare in the retrieval of above-cloud aerosol optical depth? A case study-based assessment, Geophysical Research Letters AGU Publications, RL 10.1002/2013GL058405, 2013.

[7]    Nakajima, T., and M. D. King (1990), Determination of the optical thickness and effective particle radius of clouds from reflected solar radiation measurements: Part 1: Theory, Journal of the Atmospheric Sciences, 47(15), 1878-1893.

[8]    Peers, F., Waquet, F., Cornet, C., Dubuisson, P., Ducos, F., Goloub, P., Szczap, F., Tarné, D., Thieuleux, F.: Absorption of aerosols above clouds from POLDER/PARASOL measurements and estimation of their direct radiative effects, Atmos. Chem. Phys., 15,  4179-4196, doi:10.5194/acp-15-4179-2015, 2015.

[9]    Wang, P., P. Stammes, R. van der A, G. Pinardi, and M. van Roozendael, FRESCO+: An improved O 2 A-band cloud retrieval algorithm for tropospheric trace gas retrievals, Atmos. Chem. Phys., 8(21), 6565–6576, doi:10.5194/acp-8-6565-2008, 2008.

[10]   Yu, H., et al (2006), A review of measurement-based assessments of the aerosol direct radiative effect and forcing, Atmospheric Chemistry and Physics, 6, 613-666, doi:10.5194/acp-6-613-2006, 2006.